

# We are IntechOpen, the world's leading publisher of Open Access books Built by scientists, for scientists

6,900

Open access books available

186,000

International authors and editors

200M

Downloads

Our authors are among the

154

Countries delivered to

TOP 1%

most cited scientists

12.2%

Contributors from top 500 universities



WEB OF SCIENCE™

Selection of our books indexed in the Book Citation Index  
in Web of Science™ Core Collection (BKCI)

Interested in publishing with us?  
Contact [book.department@intechopen.com](mailto:book.department@intechopen.com)

Numbers displayed above are based on latest data collected.  
For more information visit [www.intechopen.com](http://www.intechopen.com)



# Articular Cartilage Regeneration with Stem Cells

Khay-Yong Saw<sup>1</sup>, Adam Anz<sup>2</sup>, Kathryne Stabile<sup>2</sup>, Caroline SY Jee<sup>3</sup>,  
Shahrin Merican<sup>1</sup>, Yong-Guan Tay<sup>1</sup> and Kunaseegaran Ragavanaidu<sup>4</sup>

<sup>1</sup>Kuala Lumpur Sports Medicine Centre,

<sup>2</sup>Wake Forest University Baptist Medical Center,

<sup>3</sup>The University of Nottingham Malaysia Campus;

<sup>4</sup>Clinipath, Klang

<sup>1,3,4</sup>Malaysia

<sup>2</sup>USA

## 1. Introduction

Cartilage defects continue to be a clinical challenge as regards to articular cartilage regeneration. The structure and function of articular cartilage leads to non-healing lesions after injury occurs. Well-established arthroscopic methods utilize controlled healing with marrow stimulation or transferring of non-injured cartilage to areas of injury. These include: microfracture, chondral drilling, osteochondral autograft transfer system, osteochondral allograft transplant, and autologous chondrocyte implantation. However, more often than not the treatments result in the formation of fibrocartilage and similar results within all methods with no clear superior modality (Jakobsen et al, 2005; Lubowitz et al, 2007; Magnussen et al, 2008; Nakamura et al, 2009). Recent study has investigated synthetic and biologic adjuncts to current methodology, including the use of: hyaluronic acid (HA), platelet rich plasma, mesenchymal stem cells (MSC) and peripheral blood progenitor cells (PBPC). Cell therapy has produced exciting results in animal models and has been shown to regenerate hyaline cartilage clinically in the knee joint. Our current method utilizes arthroscopic subchondral drilling of cartilage lesions in combination with a postoperative adjunct treatment involving: stimulation of the release of PBPC with filgrastim, harvest of PBPC with apheresis, and postoperative intraarticular injection of PBPC in combination with HA. Our early results lead us to the conclusion that cell therapy will have an integral part in the future treatment of cartilage damage as well as other potential orthopedic, surgical, and medical applications.

## 2. Anatomy of articular cartilage

Understanding the form and function of articular cartilage is the cornerstone to developing successful treatments for articular cartilage damage. Articular cartilage is a tissue that bears load and forms the articulating surfaces of diarthrodial joints. Articular cartilage dissipates loads, has low friction, provides lubrication, and can last up to 8 decades.

Articular cartilage is predominately composed of extracellular matrix (ECM) with a sparse population of chondrocytes that help to maintain the ECM. The major components of the

ECM are water, collagen, and proteoglycans. These combine with the chondrocytes to form the complex structure of articular cartilage which varies throughout its depth. The structure of articular cartilage is typically divided into 4 zones (superficial, middle, deep, and zone of calcified cartilage). The superficial zone or tangential zone is adjacent to the joint cavity and forms a gliding surface. The superficial zone is characterized by thin collagen fibrils that are aligned parallel with the articular surface. This zone also has disk shaped chondrocytes, low proteoglycan content, with high collagen and water contents. The middle (transitional) zone is characterized by large diameter collagen fibers which are oriented obliquely, round chondrocytes, and an increased proteoglycan content. The deep (radial) zone has the highest proteoglycan content with collagen fibers oriented perpendicular to the joint surface. The chondrocytes in the deep zone are round and organized into columns. The deepest layer is the zone of calcified cartilage and separates the hyaline cartilage from the subchondral bone. This zone is characterized by collagen fibrils that are radially aligned with round chondrocytes that are buried in calcified matrix. This zone has a low concentration of proteoglycans and a high concentration of calcium salts (Fig 1).

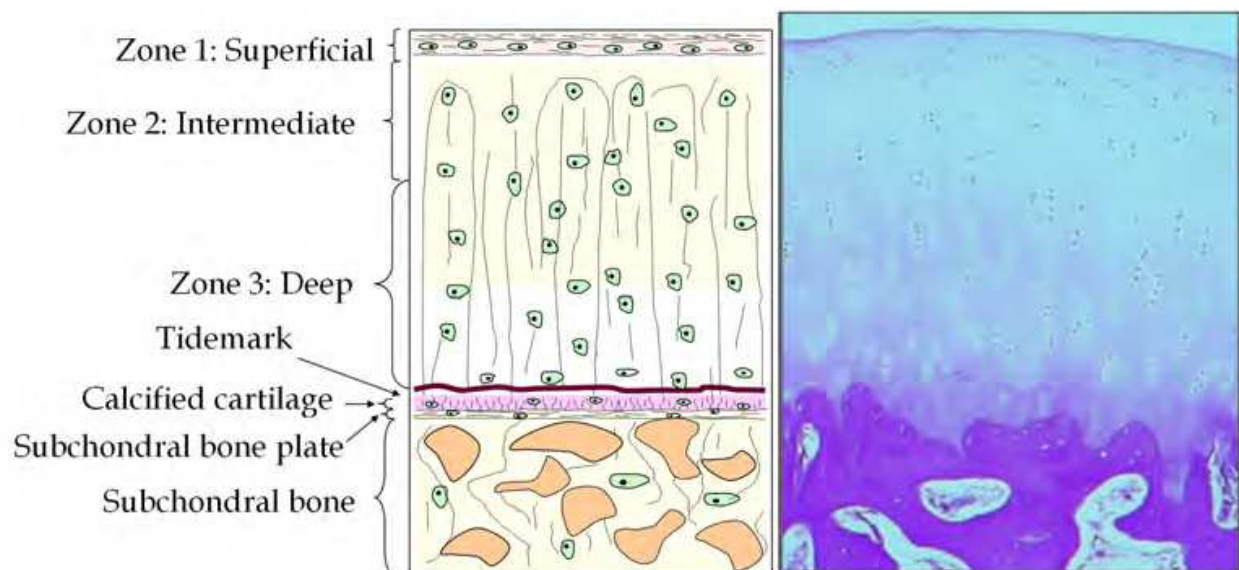


Fig. 1. This figure illustrates the zones of hyaline cartilage: superficial, middle, deep, and zone of calcified cartilage. Lacunae are present in hyaline cartilage and typically contains 1-2 chondrocytes. There is a periphery of increased proteoglycan content around each chondrocyte and lacuna.

Articular cartilage is avascular and obtains its nutrition from the diffusion of synovial fluid through the ECM and from underlying bone. Chondrocytes produce ECM components in response to chemical (growth factor and cytokines) and physical (mechanical load, hydrostatic pressure) stimuli. The ECM is composed primarily of water 65-80%, collagen (type II) 10-20%, and aggrecan 4-7%. Other components of the ECM make up less than 5% of articular cartilage. These include proteoglycans, biglycan, decorin, fibromodulin, various collagen types (V, VI, IX, X, XI), link protein, hyaluronate, fibronectin, and lipids. The role of each of these molecules is not fully understood. Collagen functions to provide shear and tensile strength to the cartilage. Proteoglycans are produced and secreted by the chondrocytes. Proteoglycans are tangled in between collagen fibers creating an ECM that inhibits the movement of water and provides compression strength of cartilage. Aggrecan

molecules for example bind with hyaluronic acid to create macromolecules (proteoglycan aggregate). These macromolecules are effectively immobilized in the collagen ECM. There tends to be a higher concentration of proteoglycans in the ECM closest to the chondrocytes. Proteoglycans are made up of repeating disaccharide subunits called glycosaminoglycans (GAG). There are 3 types of GAGs found in cartilage 1. chondroitin sulfate, 2. keratan sulfate, and 3. dermatan sulfate. Chondroitin sulfate is most abundant and with age chondroitin-4 sulfate is found to decrease while keratan sulfate increases. These changes with age or arthritis can directly affect the properties of the cartilage. For example, with age, articular cartilage has decreased water content but with osteoarthritis it has increased water content (Mankin et al, 2000).

### 2.1 Histology of cartilage

To image articular cartilage, standard hematoxylin and eosin (H&E) is sufficient to visualize cartilage damage and clinical use (Fig 2). However, additional stains can provide more specific information about the ECM, proteoglycans, and chondrocytes. For proteoglycans cationic dyes such as Safranin-O and Alcian blue are typically used. Safranin-O stains polysaccharides (both carboxylated and sulfated) orange. Alcian blue can stain for both types of polysaccharides (pH 2.5) or be more specific for sulfated polysaccharides (pH 1.0) such as chondroitin sulfate, turning them turquoise (Horvai 2011). A Trichrome (Gomori or Masson's) stain highlights the orientation of collagen fibrils with a bright blue stain, while staining cytoplasm and other proteins red. Additionally, elastin fibers which are abundant in elastic cartilage are typically visualized with a silver stain such as a Verhoeff stain where the fibers stain black. Cartilage staining can provide clear visualization of the cartilage profile in a specific location, however it is more qualitative than quantitative. To obtain more quantitative measurements of protein content Polymerase Chain Reaction (PCR) and other molecular techniques are needed.

## 3. Cartilage injury

Partial and full thickness cartilage defects have a limited ability for healing. This is in part attributed to the avascular properties of cartilage, limited stem cell population, as well as the hypoxic environment of diarthrodial joints. Additionally the mechanical loads in the joint can make articular cartilage healing a challenge. The full natural history of full thickness chondral defects is not well documented in the literature. However it is thought that full thickness defects left untreated lead to joint space narrowing and degenerative arthritis (Messner & Maletius, 1996).

Cartilage injuries can occur with a twisting, shearing type injury in combination with axial loading. These defects are commonly associated with concomitant knee pathology such as meniscus tears, anterior cruciate ligament tears, medial collateral or lateral collateral ligament tears. There is a 5-10% incidence of full thickness chondral lesions following acute hemarthrosis (Noyes et al, 1980). In athletes, there is approximately a 36% prevalence of full thickness focal chondral defects, with 14% being asymptomatic (Flanigan et al, 2010).

Patients who have symptomatic chondral lesions typically present with pain localized to the compartment of injury, increased with weight-bearing of that compartment. They may also have recurrent effusions, catching, locking, or other mechanical symptoms. The physical examination typically will demonstrate crepitation, joint effusion, tenderness along ipsilateral



joint line, signs of concomitant injury (meniscus or ligamentous), or malalignment. Coexisting malalignment can contribute to chondral injuries, i.e. patella maltracking, high Q angle, tight lateral patellar retinaculum, or varus/valgus alignment (Fig 3) (Freedman et al, 2004).

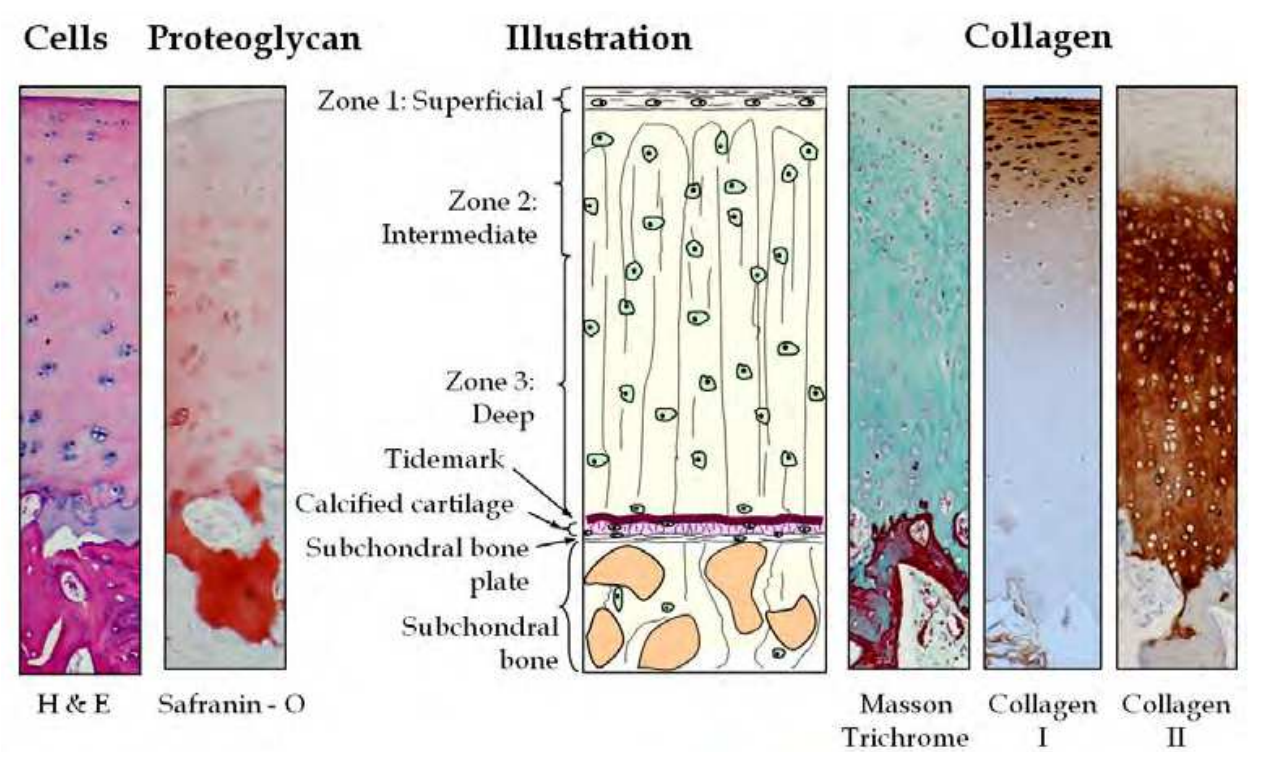


Fig. 2. This figure demonstrates how cartilage can be visualized differently with varying histological stains. From left to right: hemotoxylin & eosin (H&E) shows cellular content, Safranin-O highlights proteoglycan content, Masson’s Trichrome shows collagen fibers and orientation of fibers, and immunohistochemistry can illustrate the different collagen types. Histological stains provide visualization and qualitative analysis of cartilage.

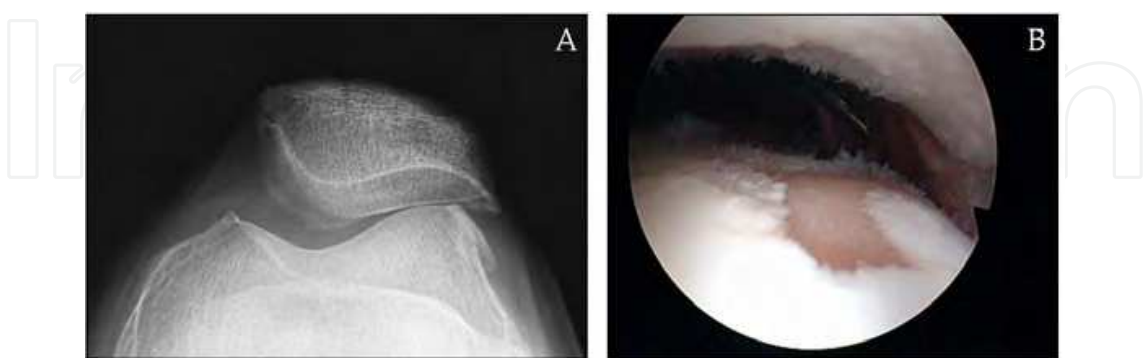


Fig. 3. Illustration of lateral patellar maltracking and its effects on chondral wear in the patellofemoral joint. (A) Radiograph with lateral patella maltracking, and (B) arthroscopic view showing chondral injury in a patient with lateral patella maltracking and the “kissing lesion” associated.

#### 4. Cartilage regeneration methods

In 1959, abrasion arthroplasty was developed by Pridie to address chondral defects (Pridie, 1959). Originally developed as an open procedure, it was later adapted for arthroscopy by Johnson (Johnson, 1986). Today, abrasion arthroplasty is used primarily for osteoarthritic knees. However, for small focal chondral defects, microfracture is most commonly used.

Microfracture is a marrow stimulating technique that penetrates the subchondral bone in the cartilage defect (Fig 4). This allows marrow to communicate with the cartilage defect populating it with MSC, inflammatory mediators, and blood. This technique is simple to perform and has good to excellent clinical results (Gill, 2000; Steadman et al, 2003; Asik et al, 2008). Postoperative management requires prolonged non-weight-bearing (4 to 6 weeks) followed by the use of continuous passive motion. However, microfracture generates fibrocartilage in the defect and has a shorter functional lifespan compared with hyaline cartilage (Menche et al, 1996; McGuire et al, 2002; Steinwachs et al, 2008).

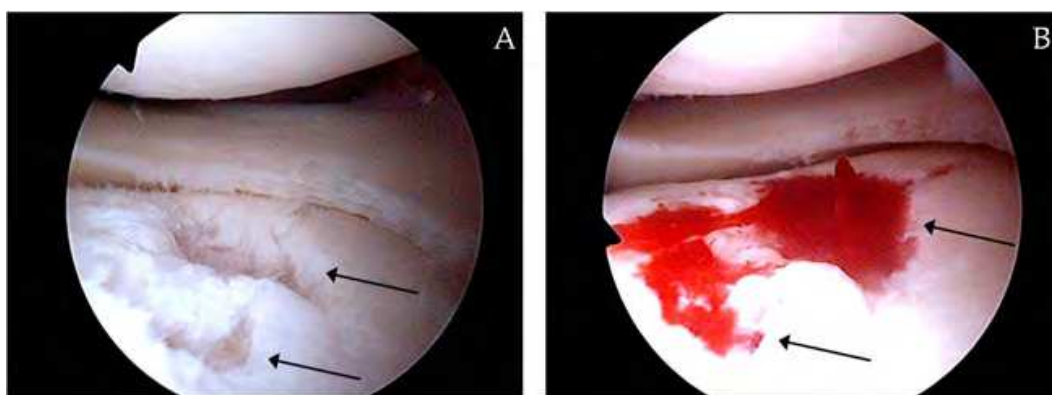


Fig. 4. Marrow stimulation with: (A) microfracture provides a source of (B) blood cells and bone marrow mesenchymal stem cells for cartilage regeneration. Healing response typically results in fibrocartilage formation.

Other techniques to address focal cartilage defects are osteoarticular transfer system with auto/allograft transplantation (OATS). This technique involves transplanting the defect with an intact cartilage and subchondral bone plug. This technique is typically used for small to medium sized lesions (0.5-3cm<sup>2</sup>) (Fig 5). If a larger area is to be addressed a mosaicplasty is performed with multiple plugs. The main disadvantages are donor site morbidity, breakdown between the implanted cartilage and subchondral bone, gaps that remain between plugs, as well as technical difficulty.

More recently autologous chondrocyte implantation (ACI) was developed to regenerate cartilage closer to hyaline cartilage. This technique can be used for larger defects (2-10 cm<sup>2</sup>), in patients who are symptomatic, and primarily located on the femoral condyles. To perform ACI requires 2 stages. The first stage involves harvesting cartilage from a biopsy to acquire cartilage cells. These cells are cultured to produce expanded autologous chondrocytes, which are subsequently implanted in the defect and held in place with a periosteal patch or collagen sheet sewn in place and sealed with a fibrin glue (Gooding et al, 2006). The postoperative course is challenging with a prolonged course of protected weight-bearing and continuous passive motion for 4 to 6 weeks. It can take up to 1-1.5 years for larger lesions to fill in. Second generation ACI is currently undergoing development to overcome the technical disadvantages of the first generation. Second generation ACI uses

tissue engineered 3- dimensional scaffolds that are seeded with autologous chondrocytes to promote cartilage regeneration. Despite continued technological improvements, clinical outcomes have yielded primarily symptomatic relief with fibrocartilage generation. The regeneration of long lasting hyaline cartilage continues to be a challenge (Ossendorf et al, 2007; Tuan, 2007).

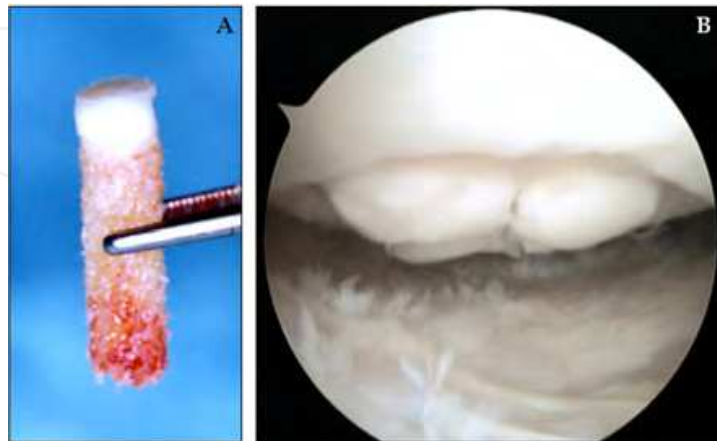


Fig. 5. Transfer system with auto/allograft transplantation (OATS) is illustrated in this figure with (A) harvesting and (B) second-look at one year showing chondral defects between the osteochondral plugs.

## 5. Adjuncts to current methods

Recent literature has illustrated that postoperative additions of HA to arthroscopic cartilage procedures yield better results (Johnson 1986; Kujawa & Caplan 1986; Gill, 2000; Freedman et al, 2004; Jakobsen et al, 2005; Gooding et al, 2006; Lee et al, 2007; Kang et al, 2008; Horvai et al, 2011; Fortier et al, 2011). High molecular weight hyaluronic acid is a component found in synovial fluid that has been investigated as adjunct for full thickness cartilage injury, microfracture, mesenchymal stem cells, and osteochondral allografting. Studies indicated that hyaluronic acid may play a role with differentiation of stem cells to chondrocytes, decreased joint inflammation, increased proteoglycan content, improved histologic scores, defect filling and incorporation, as well as decreased friction in the joint.

Another approach in attempts to regenerate hyaline cartilage are to use cells delivered either seeded on a matrix or transplanted to the defect similar to ACI. There are many cells that have been investigated, these include: mesenchymal stem cells (adipose versus bone marrow derived), chondrocytes, periostium, perichondrium. Short term results for these cellular based treatment modalities have been positive. However, long term clinical results are uncertain and have had limitations. Chondrocytes for example, lose chondrocyte phenotype with monolayer cell culture expansion and change to a fibroblastic appearance.

When chondrocytes are combined with matrix/scaffold materials the result is predominately fibrocartilage. Perichondral/periosteal cells also have chondrogenic potential in vitro and in vivo when seeding matrices. However limitations have included, variable results, the need for 2 surgeries for harvest and implantation, and instability of repair tissue. Mesenchymal stem cells either adipose derived or bone marrow derived have multilineage potential and in the appropriate microenvironment will differentiate to chondrocytes. In vivo studies have yielded short term success in generating hyaline cartilage. However, long

term results and stability of the repair tissue remain to be demonstrated (Steinert et al, 2007). Stem cell transplantations are widely used in treatments where they are induced to differentiate into specific cell types required in repairing damaged or destroyed cell tissues (Chung et al., 2006). Stem cells are capable of differentiating in vitro and in vivo along multiple pathways that include bone, cartilage, cardiac and skeletal muscle, neural cells, tendon, adipose, and connective tissue (Panagiota et al., 2005). There has been a vast and increasing interest in the research and application of human mesenchymal stem cells (hMSC) in the area of regenerative medicine over the last decade. The reasons are due to the multipotency and stability of the cellular characteristics of hMSC. However, stem cell growth and differentiation, particularly for hMSC, requires a complex and tightly regulated system consisting of medium, growth factors and serum components.

hMSC has been studied for many years and there are a set of tests that can be performed as the minimal criteria for defining multipotency of mesenchymal stromal cells (Dominici et al, 2006). These are:

1. Plastic adherent assessment: hMSC is known to be able to adhere to plastic and hence the first observation is whether the cultured hMSCs exhibit the "plastic-adherent" behaviour using standard tissue culture flasks at standard culture conditions.
2. Surface antigen expression: more than 95% of the hMSC population is to express positive for CD105, CD73 and CD90. These can be easily measured using flow cytometry. In addition, the cells have to show negative expression (less or equal to 2%) of CD45, CD34, CD14 or CD11b, CD79a or CD19 and HLA class II.
3. Multipotent differentiation potential assessment: One of the criteria that defines hMSC is that the cells must differentiate under in vitro culture conditions to osteoblasts, adipocytes and chondroblasts. The identification of these differentiated cells can be done via Alizarin Red or von Kossa staining (for osteoblast), Oil Red O (for adipocytes) and Alcian blue or immunohistochemical staining for collagen type II (for chondroblasts).

There are numerous reports in the literature using MSC to regenerate bone and cartilage. A few of the examples are outlined in Table 1 below. Generally, the use of MSC will involve either direct injection or incorporation with a scaffold or matrix to aid delivery of the cells to the intended site (Nöth et al, 2008). Nevertheless, not all cases use MSC directly, most often the MSC are differentiated in vitro for various purposes. This involves some form of benchtop work either with isolation of cells or culture expansion thus leading to increased costs.

The literature has not shown any strong evidence that any of the above methods actually generated fully function cartilage matching the original cartilage although evidence has suggested an improvement of the condition with these treatments. It is theorized that MSC have an unknown number of bioactive molecules that are immunoregulatory and able to promote regenerative activities (Chen et al 2006 & Uccelli et al, 2007). There are cases whereby MSC are used with or without a matrix as a vehicle to deliver gene therapy site specific. However, these are still experimental and will not be covered in this chapter.

Additional approaches to regenerate hyaline cartilage are to adjunct bone marrow stimulation with growth factors and hyaluronic acid which is rich in glycosaminoglycans and provide the building blocks necessary for cartilage regeneration. Investigators are beginning to evaluate platelet rich plasma (PRP). There are numerous proteins found in platelets including growth factors involved in the healing response such as platelet derived growth factor (PDGF), vascular endothelial growth factor (VEGF), transforming growth



factor (TGF-M1), fibroblast growth factor (FGF). Early research has shown that mesenchymal stem cells and chondrocytes exposed to PRP have increased cell proliferation and production of proteoglycans and collagen type II (Fortier et al, 2011). In a clinical cohort comparing hyaluronic acid with PRP injections, PRP had improved pain scores (Sanchez et al, 2008). However, the quality and longevity of the repair tissue generated by the adjunct of PRP is still unproven.

Applications	Techniques	Scaffolds used	Status
Growth plate cartilage injury	Autologous mesenchymal stem cells seeded onto Gelform scaffold containing TGF-β1 growth factor, then transplanted to injury site (McCarty et al, 2010)	Gelform	Animal (ovine) study
Large cartilage defects	Direct intra-articular injection of autologous mesenchymal stem cells suspended in hyaluronic acid ( Lee et al, 2007)	None	Animal (porcine model)
Osteoarthritis	Direct intra-articular injection of autologous mesenchymal stem cells in a dilute solution of hyaluronic acid ( Murphy et al, 2003)	None	Animal (Caprine model)
Full-thickness cartilage defects	Autologous mesenchymal stem cells seeded with collagen type I hydrogels (Wakitani et al , 2004)	Collagen type I hydrogels	Human

Table 1. Examples of clinical applications of hMSC

6. Arthroscopic subchondral drilling augmented with peripheral blood progenitor cells (PBPC)

Our laboratory has had increased interest in the used of peripheral blood progenitor cells (PBPC) over the use of bone marrow derived progenitor cells (BMPC). A study report published in April 2011 by the first author’s group (Saw et al, 2011) confirmed that articular hyaline cartilage regeneration was possible with arthroscopic subchondral drilling followed by postoperative intraarticular injections of autologous PBPC in combination with HA.

Treatment involving progenitor cells stems from the hematology/oncology profession: Given the potential morbidity associated with iliac crest harvest, cell collection for bone marrow repopulation now involves mobilization of multipotential progenitor cells through hormonal stimulation and collection via a peripheral automated cell separator machine. This process, commonly referred to as apheresis, has potential for increased magnitude of harvest. Studies involving review of healthy donors have shown this to be a safe and effective procedure for the production and harvest of cells (Ceselli et al, 2009 & Holig et al, 2009). Recent study into the properties of these PBPC has shown that they are similar to embryonal stem cells in that they express transcription factors specific to pluripotential cells, have proliferative potential, have the ability to differentiate into a multitude of cell types, and are more immature than

BMPC (Ceselli et al, 2009). In addition, when injected subcutaneously into mice, these cells were found to migrate to multiple organs and integrate and function as the surrounding cells (Ceselli et al, 2009). In addition to implementing evidence from recent animal studies, we have sought to make use of clinical evidence regarding the potential and safety of PBPC, preferring to use PBPC as opposed to BMPC because of the ease of harvest, decreased harvest-site morbidity, and increased potential with these cells (Ceselli et al, 2009; Holig et al, 2009 & Ordemann et al, 1998). In the clinical setting, we prefer to use PBPC as opposed to BMPC due to the ease of harvest and the increased potential with these cells. Subsequently, we have developed a method involving standard marrow stimulation in the form of subchondral drilling and novel postoperative intraarticular injections of autologous PBPC in combination with HA to regenerate articular cartilage.

## 7. Authors preferred method

### 7.1 Evolution of technique

Arthroscopic surgeons are regularly faced with the challenges of providing a satisfactory end result for the treatment of chondral lesions. Prior to the development of the current method, the first author was treating chondral lesions with standard subchondral drilling followed by postoperative intraarticular injections of hyaluronic acid (HA). This being a variant of marrow stimulation technique, produces fibrocartilage which is not as resilient as the original hyaline cartilage. The newly regenerated fibrocartilage gradually deteriorated with time. Since Year 2005, the first author has been dissatisfied with the inconsistent end results following this method of cartilage repair as shown in Fig 6.

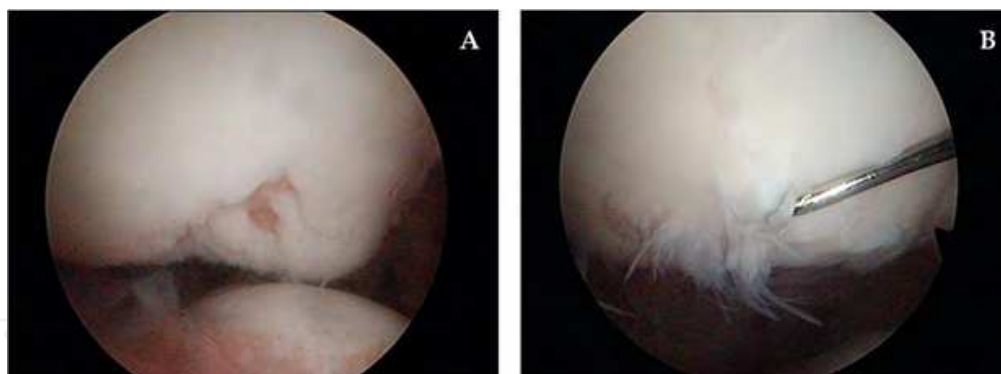


Fig. 6. Intraoperative view after subchondral drilling of the lateral patella facet - right knee (A). Second-look at 18 months (B) showing partial coverage of the defect with fibrocartilage.

At the same time, veterinary surgeons have shown that injections of bone marrow aspirate into race horse's flexor tendon injuries resulted in satisfactory healing (Pacini et al, 2007; Taylor et al, 2007; Thomas et al, 2008 & Violini et al, 2009). This gave rise to the idea of utilizing stem cells in the knee joint to initiate articular cartilage repair after subchondral drilling.

A literature search suggests that the mesenchymal stem cell (MSC) is a better alternative to the chondrocyte as it is a less differentiated cell and is capable of differentiating into both bone and articular cartilage. As most chondral lesions involve both these components, cells that are capable of forming both bone and cartilage should theoretically

be able to regenerate into tissue that will integrate better with the surrounding native structures. This may minimize of delamination which is occasionally seen by the autologous chondrocyte implantation (ACI) technique. Fig 7 shows the potential differentiation process of MSC.

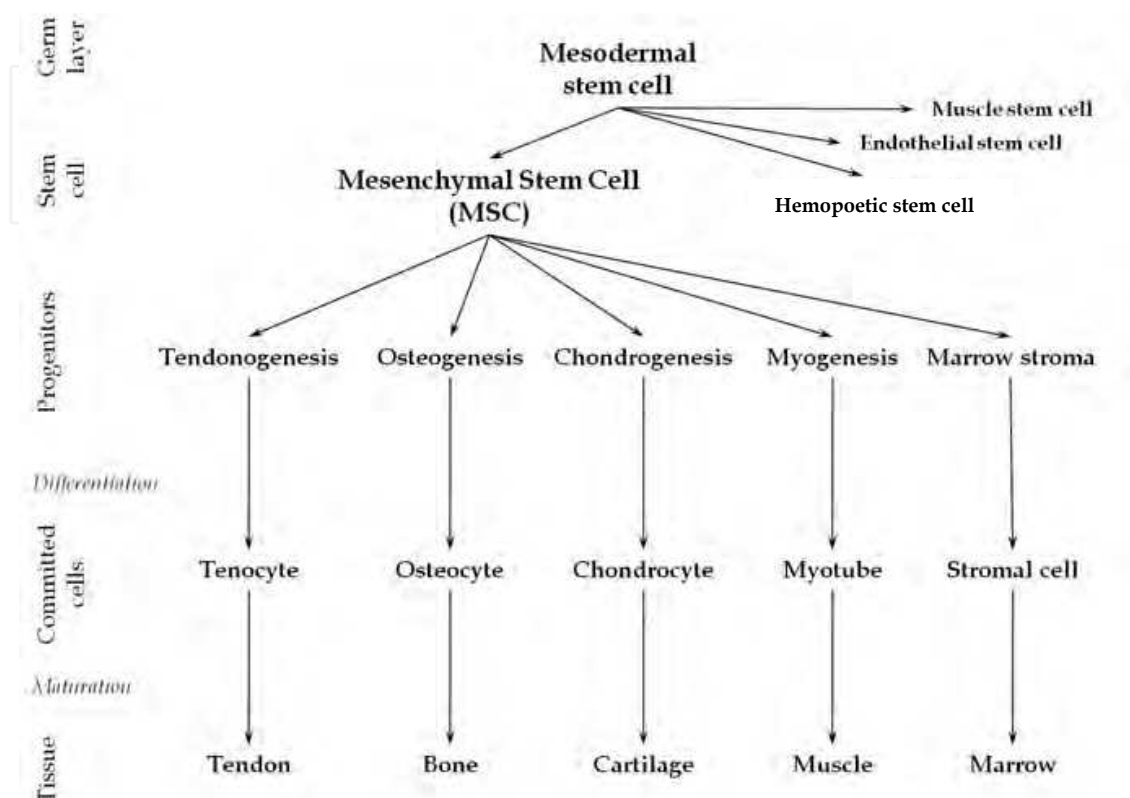


Fig. 7. Potential differentiation process of MSC.

Open surgery does not appeal to arthroscopic surgeons. The ideal method of articular cartilage repair would be a single arthroscopic procedure followed by an adjunct cell therapy which could be performed in the out-patient setting. Obviously the desired end result should be the regeneration of the original hyaline cartilage with clinical improvement. The arthroscopic surgeon's wish list for chondrogenesis is listed below:

- Single arthroscopic procedure
- Able to treat multiple/kissing lesions
- Applicable in large osteochondral defects
- Simple delivery - intraarticular injections
- Scaffold free
- Treat associated injuries
- Regeneration of soft tissues
- Cost effective
- Hyaline cartilage regeneration

## 7.2 Animal model

The following work has been published in *Arthroscopy: The Journal of Arthroscopic and Related Surgery*, Vol 25, No 12 (December), 2009: pp 1391-1400 (Saw et al, 2009). An excerpt of the published work is described.

In the animal model, we wished to find out whether postoperative intraarticular injections of autologous marrow aspirate (MA) and HA after subchondral drilling could result in a better cartilage repair.

A 4 mm full thickness articular cartilage defect was created in the stifle joint, followed by subchondral drilling as shown in Fig 8. The animals were divided into three groups: group A (control), no injections; group B (HA), weekly injection of 1 mL of sodium hyaluronate for 3 weeks; and group C (HA + MA), similar to group B but with 2 mL of autologous MA in addition to HA. MA was obtained by bone marrow aspiration, centrifuged, and divided into aliquots for cryopreservation. 15 animals were equally divided between the groups and sacrificed 24 weeks after surgery, when the joint was harvested, examined macroscopically and histologically (Fig 9).

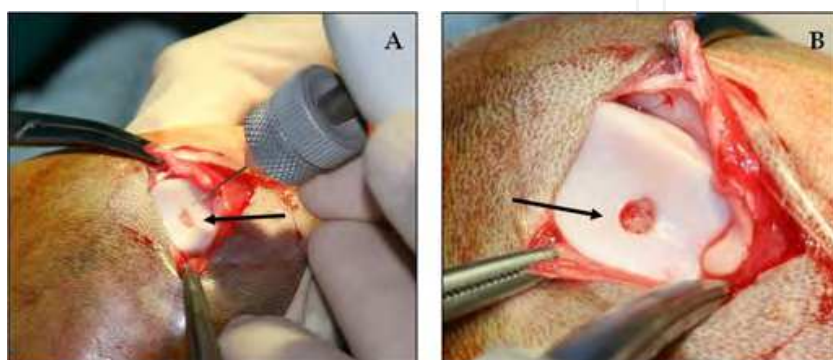


Fig. 8. (A&B) A 4mm full thickness articular cartilage defect was created in the stifle joint, followed by subchondral drilling.

### 7.2.1 Macroscopic findings

The chondral defects were covered with repair tissue in all groups, without evidence of synovitis or synovial thickening (Fig 9). In group A the defects were covered with semitransparent tissue having recognizable margins but with an irregular surface. A similar appearance was seen in group B goats. In group C the defect coverage was almost complete, and the color of the repair tissue was indistinct from surrounding cartilage. The surfaces were smooth and appeared level with adjacent normal cartilage.

### 7.2.2 Histologic findings

Under H&E staining, scar tissue was present in group A, which was characterized by a disordered arrangement of fibroblasts in an edematous stroma (Fig 9). The interface of scar tissue with subchondral bone was marked by the presence of dilated capillaries and venules. In group B scar tissue was less pronounced, and islands of hyaline-like cartilage were seen at the interface with subchondral bone and also adjacent to normal cartilage at the defect margins. Edema was also less marked than in the control group. In group C there was chondrogenesis with evidence of hyaline cartilage formation. The hyaline cartilage also showed features of maturation as evidenced by a linear arrangement of chondrocytes extending from the subchondral bone toward the surface. No edema was seen in this group. With Safranin-O staining, proteoglycans were notably absent from the repair tissue in group A. In group B proteoglycans were seen only at the base and sides of the defect in the same distribution as the hyaline-like cartilage. In group C there was marked proteoglycan accumulation in the deeper layers, excluding the perichondrium, which normally does not contain proteoglycans.



Under collagen staining, the scar tissue in group A was found to contain only type I collagen, with an absence of staining for type II collagen. In group B type I collagen staining in the repair tissue was less pronounced, with light staining for type II collagen around the areas of hyaline-like cartilage. In group C type I collagen staining was found only in the perichondrium, whereas the deeper cartilage stained strongly for type II collagen.

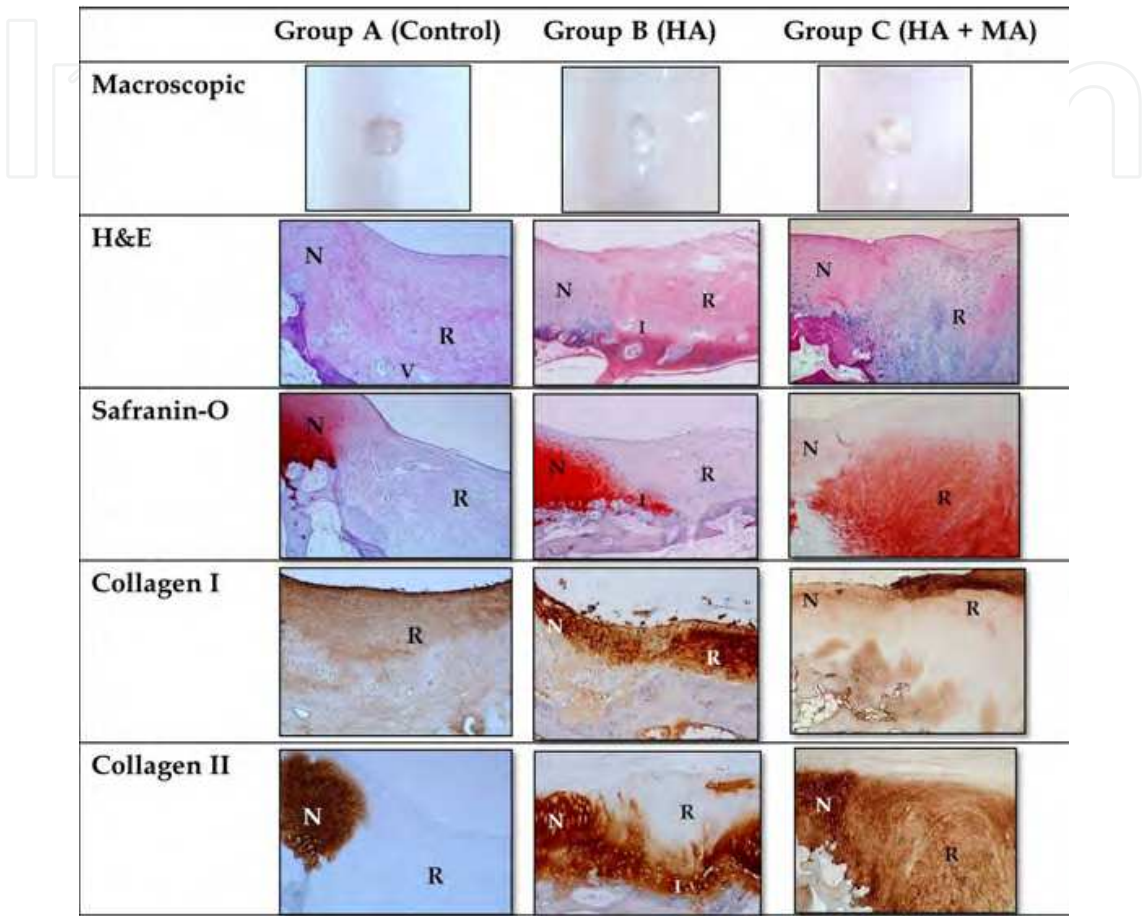


Fig. 9. Macroscopic and histologic findings for representative subjects from all 3 groups. (N, normal cartilage; R, repair cartilage; V, dilated capillaries and venules; I, islands of hyaline-like cartilage).

7.2.3 Discussion on the animal model

Penetration of the subchondral bone was shown to release the underlying marrow, which initiated repair of the chondral defect with fibrocartilage in a pattern that was observed in group A animals. The reason why fibrous tissue forms instead of hyaline cartilage is not known, but it is likely that the local microenvironment contains paracrine factors that either promote fibrous tissue formation, inhibit cartilage growth, or both.

The addition of HA in group B animals improved the quality of repair tissue by allowing hyaline-like cartilage to form. This suggests that HA modifies the microenvironment in such a way that neutralizes these paracrine factors. The incomplete regeneration could be because of HA being only partially effective or the duration of administration being too short. It appeared that the region adjacent to subchondral bone and the interface with normal cartilage seemed to be most favorable to cartilage formation.

The combination of HA and MA in group C yielded the best results in that the repair tissue was composed of true hyaline cartilage, showing vertical orientation of chondrocyte nests and the presence of type II collagen and proteoglycans in the intermediate and deep cartilage layers, with type I collagen confined to the superficial layer and perichondrium (Fig 9). This suggests that the combination of HA and MA is most effective in neutralizing the paracrine factors, and its effects persist for the duration of the repair process. One of the essential active components in MA is likely the MSC content, given that a previous study in a porcine model showed that cultured autologous MSCs injected intraarticularly together with HA could produce the same results as in the group C animals (Lee et al, 2007).

The presence of edema in the repair tissue appears to be proportional to the degree of fibrous scarring and was most marked in group A animals. The dilated capillaries and venules at the base of the defect suggest an inflammatory process that originates in the subchondral bone. These observations indicate that the paracrine factors, which promote fibrous tissue formation, are closely related to the inflammatory process that occurs after mechanical disruption of the chondral plate and that both HA and MA may be able to suppress inflammation locally.

#### **7.2.4 Conclusion on the animal model**

This preclinical experimental study in the goat model concluded that postoperative intraarticular injections of autologous MA in combination with HA after subchondral drilling resulted in a better cartilage repair.

#### **7.2.5 Clinical relevance from the animal model**

After arthroscopic subchondral drilling, postoperative intraarticular injections of autologous progenitor cells in combination with HA may result in better articular cartilage regeneration.

### **7.3 Clinical trial**

A human clinical trial followed the preclinical animal studies. The surgical technique applied in the clinical trial involved standard marrow stimulation in the form of arthroscopic subchondral drilling and postoperative intraarticular injections of autologous peripheral blood progenitor cells (PBPC) in combination with HA. The objective of the trial was to assess whether the results of the preclinical animal model could be replicated in the human knee joint. The purpose of the clinical trial was to evaluate the quality of resultant articular cartilage regeneration. A hypothesis was made that articular hyaline cartilage regeneration was possible with this novel approach.

The early results with histology were published in *Arthroscopy: The Journal of Arthroscopic and Related Surgery*, Vol 27, No 4 (April), 2011: pp 493-506 . An excerpt of the paper is presented in the following sections (Saw et al, 2011).

#### **7.3.1 Patient selection – indication for surgery**

The diagnosis of chondral injury was made after clinical and radiologic evaluation. Chondral lesions were graded according to the International Cartilage Repair Society (ICRS) Cartilage Injury Evaluation Package (Brittberg & Peterson, 1998) The inclusion criteria were patients with ICRS grade III and IV lesions, defects of any size and number, age 18 to 60 years, deformity (lateral patella maltracking or axis correction) correctable at the time of surgery, and ligamentous instability deemed reconstructable at the same time. The exclusion criteria were patients with disease progression such that total knee arthroplasty was indicated; a history of

infected knees, gross bone defects, rheumatoid arthritis, or intraarticular corticosteroids within the previous 6 weeks; and gross valgus or varus deformity not correctable during surgery.

### 7.3.2 Surgical procedure

All surgical procedures were performed by a single surgeon (by the first author) involving standard arthroscopic techniques in the supine position without a tourniquet. Saline solution irrigation bags were chilled in an ice-water bath before use to minimize bleeding during the arthroscopic procedure. In our experience, we have had difficulty performing microfracture to the patella and areas of the plateau. For this reason, our preferred method is arthroscopic subchondral drilling modified from the principles established by Steadman et al (Steadman et al, 1999), for microfracture and Pridie (Pridie, 1959) for drilling. We begin by defining the extent of cartilage injury with a probe. A 3.5 mm full-radius shaver is used to debride loose cartilage to a stable margin; often a straight or curved arthroscopic biter is required as well. A 2 mm burr, with its guard removed, “drills” from the surface of the defect to the bone marrow, creating a conduit. The remaining area within the margin is also drilled to a depth of 5 to 10 mm. Initially, we spaced drill holes 3 to 4 mm apart. The methods have subsequently been refined such that a goal of 1 to 2 mm between drill holes is now preferred based on the results of second-look arthroscopy. It is not crucial that the subchondral drilling be performed perpendicular to the bone surface because a lesser angle of drilling capable of penetrating into the subchondral bone is sufficient. Abrasion chondroplasty up to a depth of 1 mm is performed with burring of the bony area between drill holes. The result is an extended area of bleeding bone, hence a larger surface area for the initiation of articular cartilage repair with PBPC and HA (Fig 10). The arthroscopic portals are closed with No. 3-0 nylon suture. A mixture of 20 mL of 0.5% bupivacaine hydrochloride and epinephrine, 3 mL of 1 mg/mL morphine, and 2 mL of HA (Hyalgan; Fidia Farmaceutici, Abano Terme, Italy) is injected into the operated knee at the end of the surgical procedure.

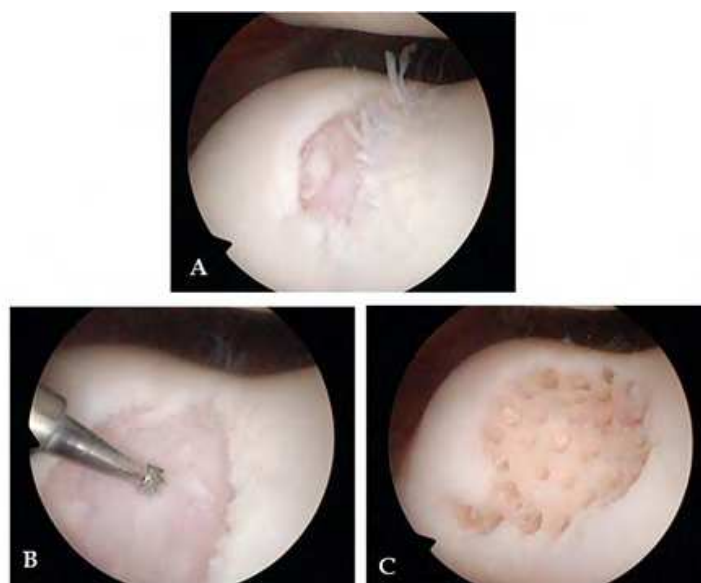


Fig. 10. Subchondral drilling. (A) A delaminated flap tear on the medial & central trochlear of a left knee. (B) A 2 mm burr with guard removed allows for drilling with light suction. (C) View after debridement, subchondral drilling and abrasion chondroplasty.



### 7.3.3 Postoperative rehabilitation

Cold therapy is initiated for one hour 2 to 3 times a day immediately in the postanesthesia period and continued throughout the first month after surgery. On the first postoperative day, continuous passive motion is used on the operated knee for a duration of 2 hours (Fig 11). This is continued daily for a period of 4 weeks. The range of motion is initially set from 0° to 30° and progresses as the clinical situation improves. Patients with subchondral drilling to the weight-bearing femorotibial joint are instructed on crutch-assisted partial weight-bearing (15 to 20 kg) for the first 4 weeks. This progresses to full weight-bearing in 6 to 8 weeks. Patients with drilling to the patellofemoral joint are allowed full weight-bearing as tolerated with restrictions from weight-bearing on stairs for the first 3 months after surgery. This is to avoid overloading the patellofemoral joint.



Fig. 11. Patients undergoing postoperative rehabilitation (A). A closer view of patients showing continuous passive motion applied on the operated knee (B).

### 7.3.4 Neupogen administration, apheresis, and cryopreservation

Human granulocyte colony-stimulating factor is a glycoprotein that regulates the production and release of functional neutrophils from the bone marrow. Neupogen contains recombinant granulocyte colony-stimulating factor and causes marked increases in peripheral blood neutrophil counts with a minor increase in monocytes within 24 hours. On postoperative days 4, 5, and 6, patients were given a morning dose of 300 micro-grams of Neupogen (Filgrastim, Amgen, Thousand Oaks, CA) subcutaneously. On postoperative day 7, autologous PBPC were collected by an automated cell separator (apheresis) via central venous access. Venous access was achieved through a femoral double-lumen catheter placed into the contralateral leg, under ultrasound guidance, performed by a trained specialist. Apheresis was performed by use of the Spectra Optia Apheresis Machine (Caridian BCT, Denver, CO). A fresh aliquot of 8 mL of PBPC was separated for fresh intraarticular injection into the operated knee. The remaining PBPC were cryopreserved in 10% dimethyl sulfoxide and divided into 4 mL cryovials for storage in liquid nitrogen at -196°C. Flow cytometry with CD34+ (hematopoietic stem cells) and CD105+ (markers for mesenchymal stem cells) was quantified. Flow cytometry was performed with a Beckman Coulter FC500 device (Beckman Coulter, Fullerton, CA). Fig 12 showing the apheresis process. The cryopreservation of the harvested PBPC in cryovials can be seen in Fig 13.





Fig. 12. A typical apheresis process.



Fig. 13. Cryopreservation of the harvested PBPC in cryovials.

**7.3.5 Intraarticular injection**

On postoperative day 7, 8 mL of the fresh PBPCs is mixed with 2 mL of HA and injected into the operated knee joint under aseptic conditions in the out-patient clinic. Prior to this, the knee is first aspirated for hemarthrosis. At weekly intervals, 8 mL (from two 4 mL cryovials) of the frozen PBPC were obtained from the laboratory, allowed to thaw to room temperature, mixed with 2 mL of HA, and injected into the operated knee joint for 4 subsequent weeks. A flow chart of the protocol for patients undergoing articular cartilage regeneration is shown in Fig 14. Table 2 shows the PBPC count of 20 recent consecutive

patients after refinement of our processing methods, showing data of fresh and frozen samples with white blood cell count, CD34+ and CD105+ counts, and cell viability.

	White Cell Count 10 <sup>3</sup> / uL	CD 34+ (10 <sup>6</sup> ) Cells per 4ml Vial		CD 105+ (10 <sup>6</sup> ) Cells per 4ml Vial		Viability %	
		Fresh	Frozen	Fresh	Frozen	Fresh	Frozen
	32.00	6.86	4.58	7.42	8.14	99.30	79.90
	24.40	1.04	0.66	9.98	14.41	99.30	89.65
	30.00	0.33	0.23	3.32	5.08	99.10	89.99
	35.60	1.03	0.74	15.44	20.33	99.01	91.97
	14.80	3.88	2.86	2.69	8.87	99.40	87.90
	33.50	0.44	0.37	8.95	7.04	99.60	95.30
	33.50	3.28	2.33	5.41	7.75	99.00	82.90
	34.80	2.02	1.34	13.60	14.01	99.50	94.04
	23.00	2.53	1.69	7.01	13.77	99.50	88.10
	37.10	2.42	1.32	3.37	5.72	98.90	88.10
	26.50	1.55	1.07	4.54	6.98	99.00	84.80
	52.10	2.76	2.17	8.89	4.56	99.40	90.30
	38.80	3.15	1.82	15.50	11.62	99.30	79.30
	32.10	0.86	0.75	12.79	6.35	98.90	91.30
	33.00	5.71	3.14	6.30	8.53	99.10	78.40
	20.00	1.02	0.62	14.80	15.40	97.80	88.40
	37.50	3.19	2.08	4.15	1.66	99.30	82.20
	26.90	2.78	1.90	1.43	4.44	99.30	82.30
	31.00	1.55	1.01	23.45	31.15	99.10	89.10
	44.60	1.16	0.67	16.62	19.40	98.50	91.80
AVERAGE	32.06	2.38	1.57	9.28	10.76	99.12	87.29

Table 2. Example of 20 consecutive PBPC counts from patients following 3 neupogen injections. Data of fresh and frozen samples with white cell count, CD34+ and CD105+ counts, and cell viability.

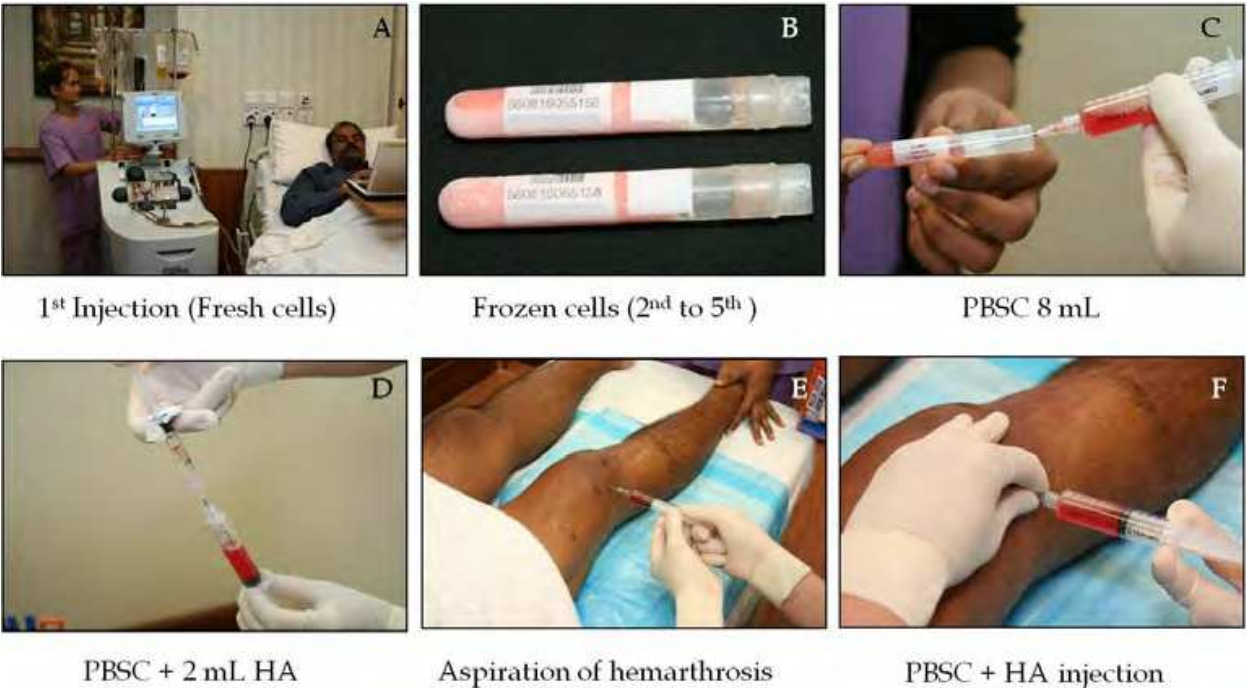


Fig. 14. Flow chart showing the standard protocol for articular cartilage regeneration with PBPC and HA.

Fresh cells are used preferably for the first injection because of a mean viability of 99% compared with frozen cells, which have a mean viability of 87%. It should be noted that 8 mL of PBPC injected into the operated knee has a mean of 20 million CD105+ cells. Historically, the cell marker CD34+ (hematopoietic stem cells) has been used to identify functional cells for bone marrow transplant. We have begun to draw interest in CD105+ cells, because this is the marker for mesenchymal stem cells.

Five weekly injections are based on the HA protocol for osteoarthritis, as well as the suggestion from preclinical animal studies involving Bone Marrow Progenitor Cells (BMPC) that an increased number of intraarticular injections is more efficacious (Saw et al, 2009). Table 3 shows the viability of 5 consecutive frozen PBPC samples after mixing with HA. As can be seen, there is no effects of HA on the viability of the PBPC.

Frozen PBPC from -196°c Storage Tank						
Patient	Before addition of HA			After addition of HA		
	CD34+ (10 <sup>6</sup> ) Based-4ml per vial	CD105+ (10 <sup>6</sup> ) Based-4ml per vial	Viability	CD34+ (10 <sup>6</sup> ) Based-4ml per vial	CD105+ (10 <sup>6</sup> ) Based-4ml per vial	Viability
A	3.000	2.010	75.10%	3.380	6.050	77.50%
B	1.060	10.800	78.90%	0.980	3.750	83.00%
C	3.220	16.800	68.20%	2.660	8.230	68.90%
D	1.020	5.150	85.10%	0.550	2.370	86.60%
E	0.720	7.710	82.20%	0.750	2.780	84.80%
AVERAGE	1.804	8.494	77.90%	1.664	4.636	80.16%

Table 3. Cell count viability.

#### 7.4 Introduction to clinical cases

Five cases are presented here with their respective chondral biopsies and histology. These cases provided explanation to the principles of chondrogenesis in our novel approach.

The patients are part of a larger pilot study in which 180 patients who presented with chondral defects of the knee joint were recruited. Postoperatively, the clinical course of these 5 patients presented an opportunity for a second-look arthroscopy. Two patients underwent contralateral knee surgery, and one patient had removal of a Tomofix plate and screw construct (Synthes, West Chester, PA), providing an opportune setting of anesthesia for second-look arthroscopy. One patient had recurrence of discomfort attributed to a prominent osteophyte and elected for a further arthroscopic procedure. The last patient had returned to football 18 months after articular cartilage repair and sustained a torn anterior cruciate ligament of the previously treated knee. He elected for arthroscopic reconstruction, which provided an opportunity for second-look arthroscopy. Informed consent after discussion of risks and benefits, as well as local ethics committee approval, was obtained before biopsy.

##### 7.4.1 Second-look arthroscopy with chondral core biopsy

During the second-look procedures, a chondral core biopsy specimen was procured. This was performed arthroscopically with a 5.5 mm sterilized BioCorkscrew anchor driver (Arthrex, Naples, FL). Typically, a 2 mm diameter specimen of cartilage together with a core of bone up to 1 cm in length is obtained (Fig 15).

Arthroscopically, the regenerated articular cartilage appeared smooth and had excellent integration with the surrounding native cartilage without any delamination or hypertrophy. The exception was case 2, in which the drill holes over the lateral patellofemoral joint were too far apart with resultant tufts of cartilage seen between areas devoid of regenerated cartilage (Fig 16).



Fig. 15. Solid articular cartilage core biopsy with a 2 mm diameter including the underlying subchondral bone.



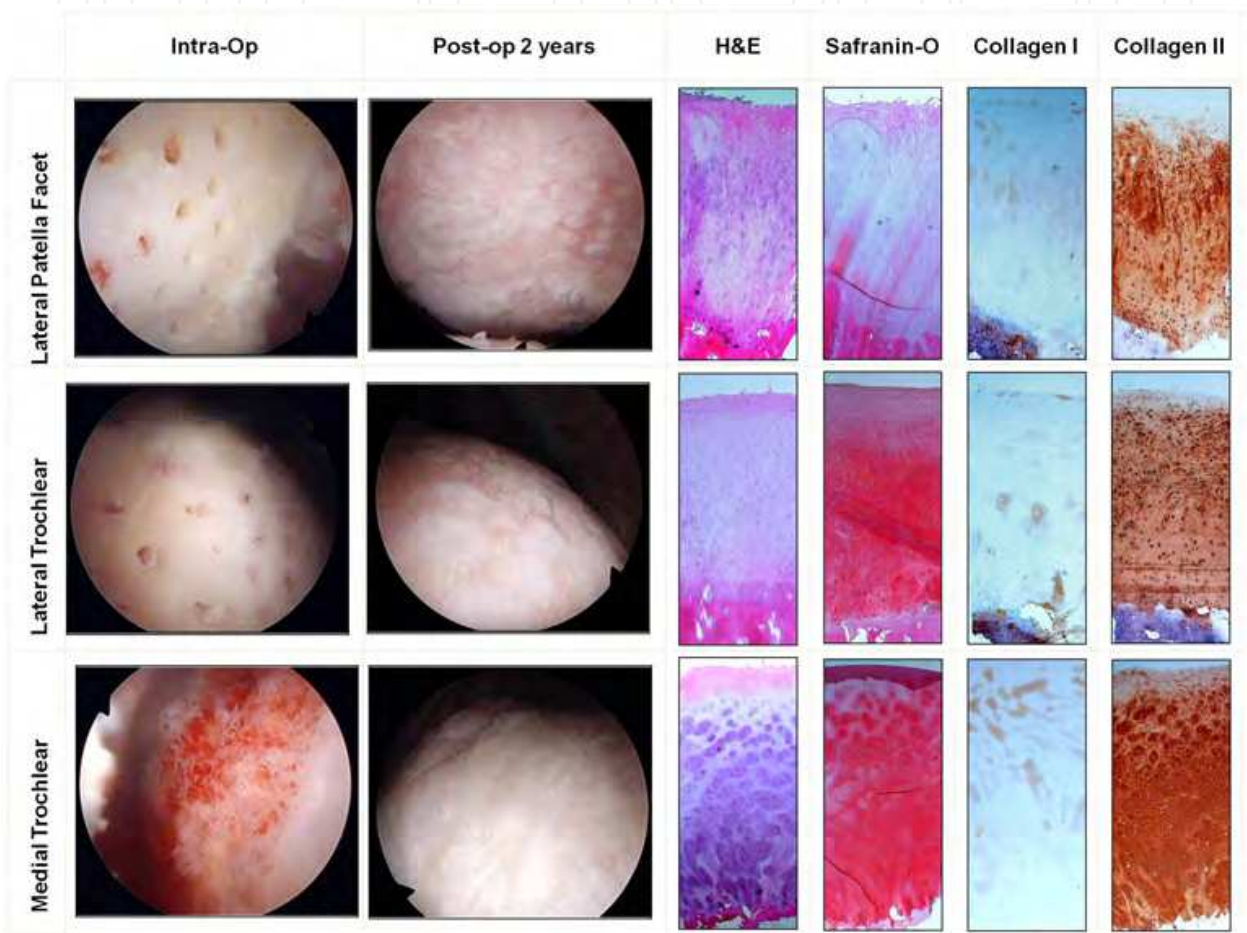


Fig. 16. 34-year-old female from Fig 22. Second-look arthroscopy from the lateral patella facet and lateral trochlear showed tufts of cartilage forming at each individual drill hole. Upon histological stains, notice the red staining with Safranin-O representing proteoglycans and the brown staining of collagen type II diffuse throughout the regenerated tissue. Collagen type I stain is minimal and localized near the superficial layers.

### 7.4.2 Histology

Histologic samples were stained as follows: hematoxylin-eosin (H&E) stain was used to visualize overall morphology, Safranin-O was used to highlight proteoglycans, immunohistochemistry staining with anti-collagen type I mouse Ab I-8H5 stain (catalog No. CP 17; Calbiochem Merck, Darmstadt, Germany) was used to highlight collagen type I, and immunohistochemistry staining with anti-collagen type II mouse monoclonal antibody Ab 3 (clone 6B3) (catalog No. MAB8887; Millipore, Billerica, MA) was used to highlight collagen type II. Optimal dilution and predigestion with pepsin were determined by the investigator with the protocol being saved by use of software of an automated immunohistochemical slide preparation system (Ventana Benchmark; Ventana Medical Systems, Tucson, AZ).

Cases 1 and 2 with gross grade IV kissing lesions are presented with multiple biopsy specimens and histologic analyses after second-look arthroscopy. Cases 3, 4, and 5 are patients with smaller isolated lesions.

**Case 1:** Biopsy was performed 22 months after the initial surgery in a 49-year-old woman with a varus deformity who underwent debridement, subchondral drilling, and an open wedge high tibial osteotomy with Tomofix fixation (Fig 17).



Fig. 17. Progressive serial weight-bearing radiographs of Case 1 with high tibial osteotomy. Notice re-appearance of the medial articulation.

Approximately 80% of the weight-bearing medial compartment had grade III and IV lesions. Weight-bearing radiographs at 8 and 18 months showed reappearance of the medial femorotibial joint space. Second-look arthroscopy of the regenerated cartilage showed a stable, smooth surface with no delamination. On probing, the regenerated cartilage had the same consistency as the surrounding normal cartilage. The second-look images and biopsy specimens are included in Fig 18.

Immunohistochemistry staining was performed to assess the collagen type I and type II content of the biopsy specimens. Specimens from the medial femoral condyle and medial tibial plateau showed the presence of collagen type I confined to the superficial layer. Collagen type II was present throughout the deeper layers. These are features of hyaline cartilage as opposed to fibrocartilage (Fig 18). Fig 19 shows a higher magnification of the histological sections from the medial tibial plateau.

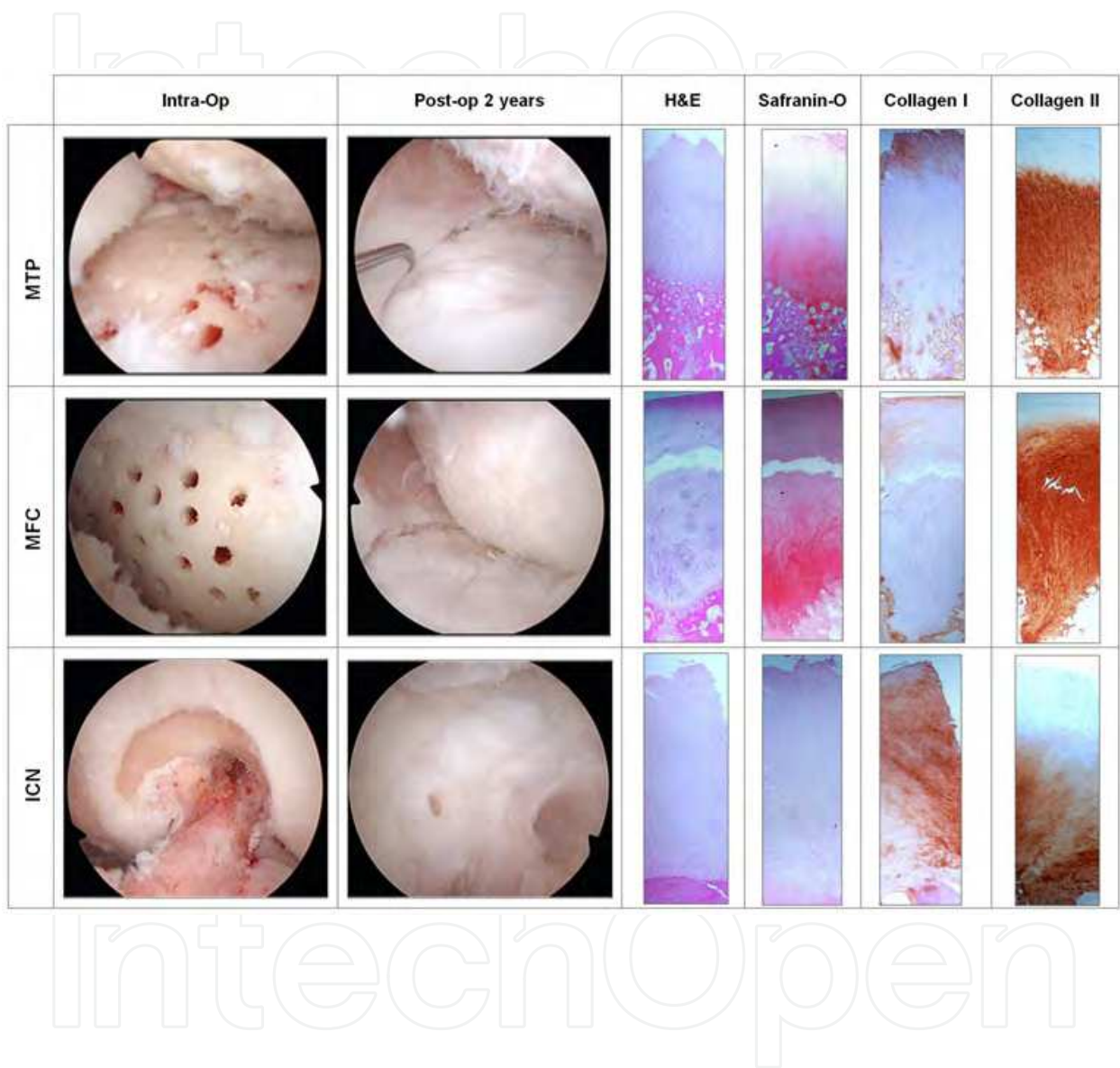


Fig. 18. Medial tibial plateau (MTP), medial femoral condyle (MFC) and intercondylar notch (ICN) biopsy results at 22 months after surgery. Biopsies from the MTP and MFC with H&E staining illustrate columnar morphology of cells with pale background. Safranin-O staining highlights abundance of proteoglycans throughout the regenerated cartilage layer. Collagen type I staining was limited to the superficial layer except in the non-weight-bearing ICN biopsy which showed a higher percentage of collagen type I and a disorganized pattern of healing. Collagen type II was concentrated in the deeper layers.

One full-thickness biopsy specimen from the medial tibial plateau captured a drill hole and adjacent bone (Fig 20). This sample shows full-thickness regenerated articular cartilage with a fairly smooth articular surface, subchondral bone, and marrow space. A streaming, linear pattern of chondrocytes is seen arising from the subchondral bone region from the area of previous subchondral drilling. Incidental findings of cartilage clusters with early ossification are also seen within the tract. The chondrocytes are involved in ongoing remodelling and are present beneath the calcified cartilage layer. A biopsy specimen from the medial femoral condyle of the patient also showed the presence of a previous drill hole lined with chondrocytes. This sample illustrated an area of regeneration undergoing ossification, showing re-establishment of the calcified cartilage layer and the tidemark (Fig 21). The tidemark is seen as an undulating basophilic line on routine H&E staining and is the point at which the articular cartilage becomes calcified. The subchondral drill defect area is replaced by the presence of chondrocytes with varying degrees of maturation surrounded by a ground substance matrix. In addition, ossification is evident with new trabecular bone formation. Ossification changes were not seen over the new hyaline cartilage formation zone.

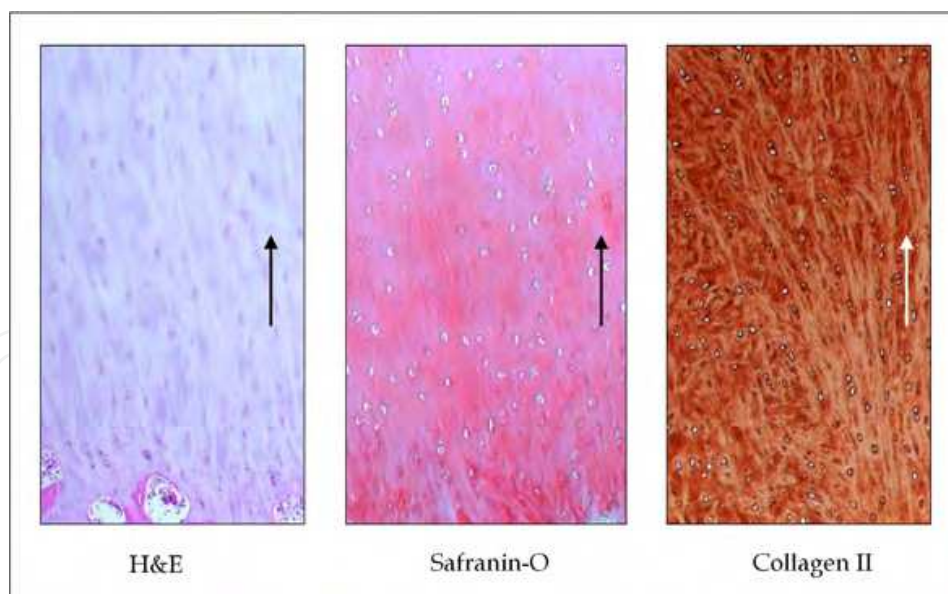


Fig. 19. Biopsy from the medial tibial plateau in case 1 showing the presence of chondrocytes and collagen fibres aligning to the axis of weight transmission with their specific stains (Original magnification X 100).



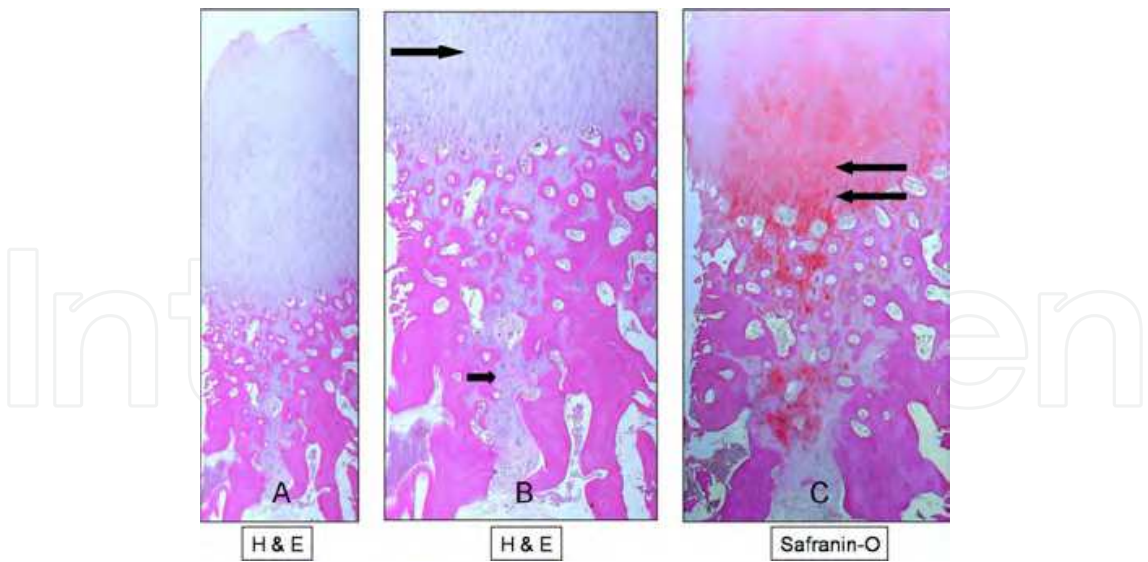


Fig. 20. (A) H&E sample as in Figure 18 from the medial tibial plateau managed to biopsy an area of previous drilling. (B) Upon higher magnification, chondrocytes appeared deep to the subchondral bone with areas of ossification. Notice the chondrocytes below the subchondral bone region beginning as immature cells (short arrow) and progressing toward the joint surface as mature chondrocytes in rows (long arrow). (C) Upon staining with Safranin-O, there was a high concentration of proteoglycans at the base of the regenerated tissue represented as red coloration (double arrow).

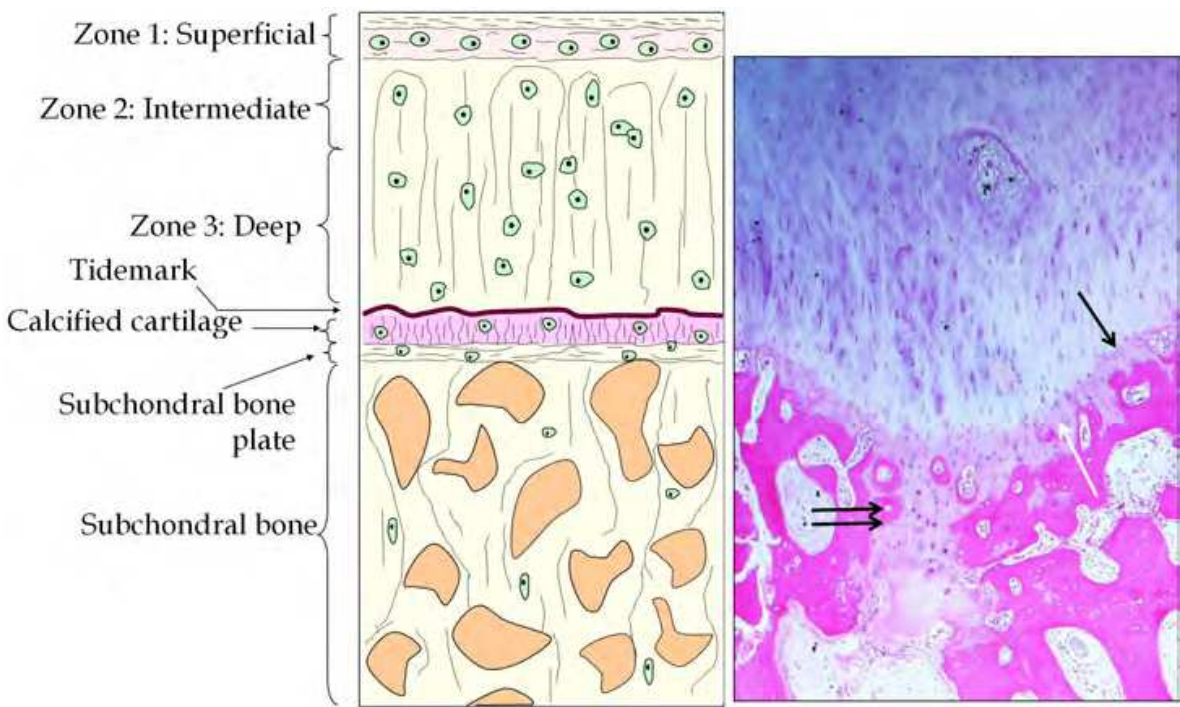


Fig. 21. A biopsy from the medial femoral condyle illustrating ossification of regenerated cartilage and the re-establishment of the calcified cartilage (white arrow) layer with tidemark (black arrow). Note the presence of chondrocytes below the calcified cartilage (double arrow) with areas of ossification.

The intercondylar notch sample was an area of previous roof-plasty and notchplasty with abrasion chondroplasty. This represents an area that is non-weight-bearing. Histologic biopsy examination here showed a mixed tissue with fibrocartilage and hyaline-like cartilage: the predominance of collagen type I, less collagen type II, and chondrocytes arranged in a more disorganized pattern. We believe that the failure of the chondrocytes to exhibit a linear streaming pattern, as seen from the medial tibial plateau and medial femoral condyle biopsy specimens, is due to the absence of stimulation from weight-bearing forces on the intercondylar notch (Fig 18).

**Case 2:** A chondral core biopsy specimen was taken 26 months after surgery in a 34-year-old woman with previous multiple open surgeries for recurrent dislocation of the patella as an adolescent. She underwent arthroscopic debridement, lateral patella release, and subchondral drilling. There were grade III and IV lesions over the entire patellofemoral joint. Preoperative merchant-view radiographs showed severe patellofemoral osteoarthritis, a large medial trochlear osteophyte, and absence of the lateral patellofemoral joint space (Fig 22). During arthroscopic surgery, the medial trochlear osteophyte was burred and subchondral drilling was performed on the entire patellofemoral joint. An immediate postoperative radiograph showed evidence of subchondral drilling. Radiographs at 6 months and 2 years showed progressive reappearance of the lateral patellofemoral joint space (Fig 22). Fig 16 contains results of the second-look arthroscopy with chondral core biopsy specimens. The lateral patella facet and lateral trochlear areas showed tufts of cartilage between areas devoid of cartilage. In contrast, the medial trochlear area that underwent the removal and burring of a large osteophyte followed by subchondral drilling showed complete coverage by newly formed articular cartilage.

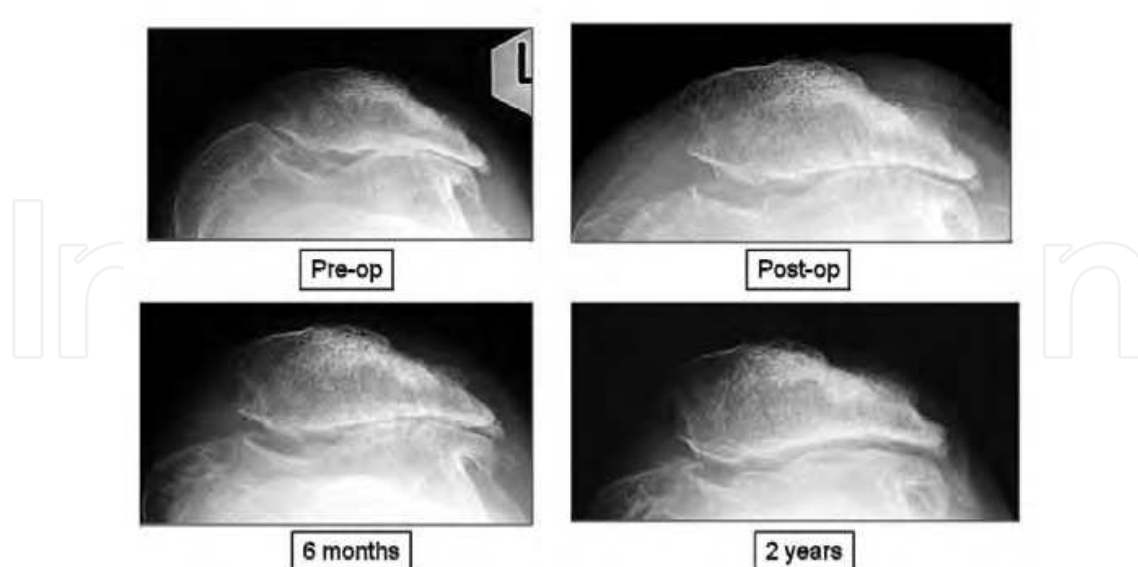


Fig. 22. 34-year-old female with recurrent dislocation of her patella as an adolescent. Immediate postoperative radiographs showed evidence of subchondral drilling while radiographs at 6 months and 2 years showed a progressive reappearance of the lateral patellofemoral articulation.

**Case 3:** A biopsy specimen was obtained 1 year after surgery from a 52-year-old woman with an isolated grade IV lesion of the lateral femoral condyle measuring 2 X 1 cm.

**Case 4:** A biopsy specimen was obtained 10 months after surgery in a 43-year-old woman with lateral patellar maltracking. There was a grade III/IV defect measuring 2.5 X 3.5 cm over the lateral patella facet. Lateral patella release was performed in addition to subchondral drilling.

**Case 5:** Biopsy was performed at 18 months after surgery in a 19-year-old man with lateral patellar maltracking and a lateral trochlear grade IV lesion measuring 0.8 cm in diameter. Subchondral drilling was performed followed by lateral patellar release (Fig 23). Chondral core biopsy specimens in cases 2, 3, 4, and 5 with histologic staining with H&E showed columnar morphology of cells with a pale blue ground substance. Safranin-O showed intense orange / red staining of the newly regenerated cartilage zone throughout the regenerated cartilage layer with a propensity toward the deeper areas of cartilage above the subchondral bone. The matrix also showed a predominance of collagen type II deposits, whereas collagen type I was minimal and located mostly over the superficial regions of the articular surface. These compositional results are features of hyaline as opposed to fibrocartilage (Kang et al, 2008; Saw et al, 2009 & Lee et al, 2007).

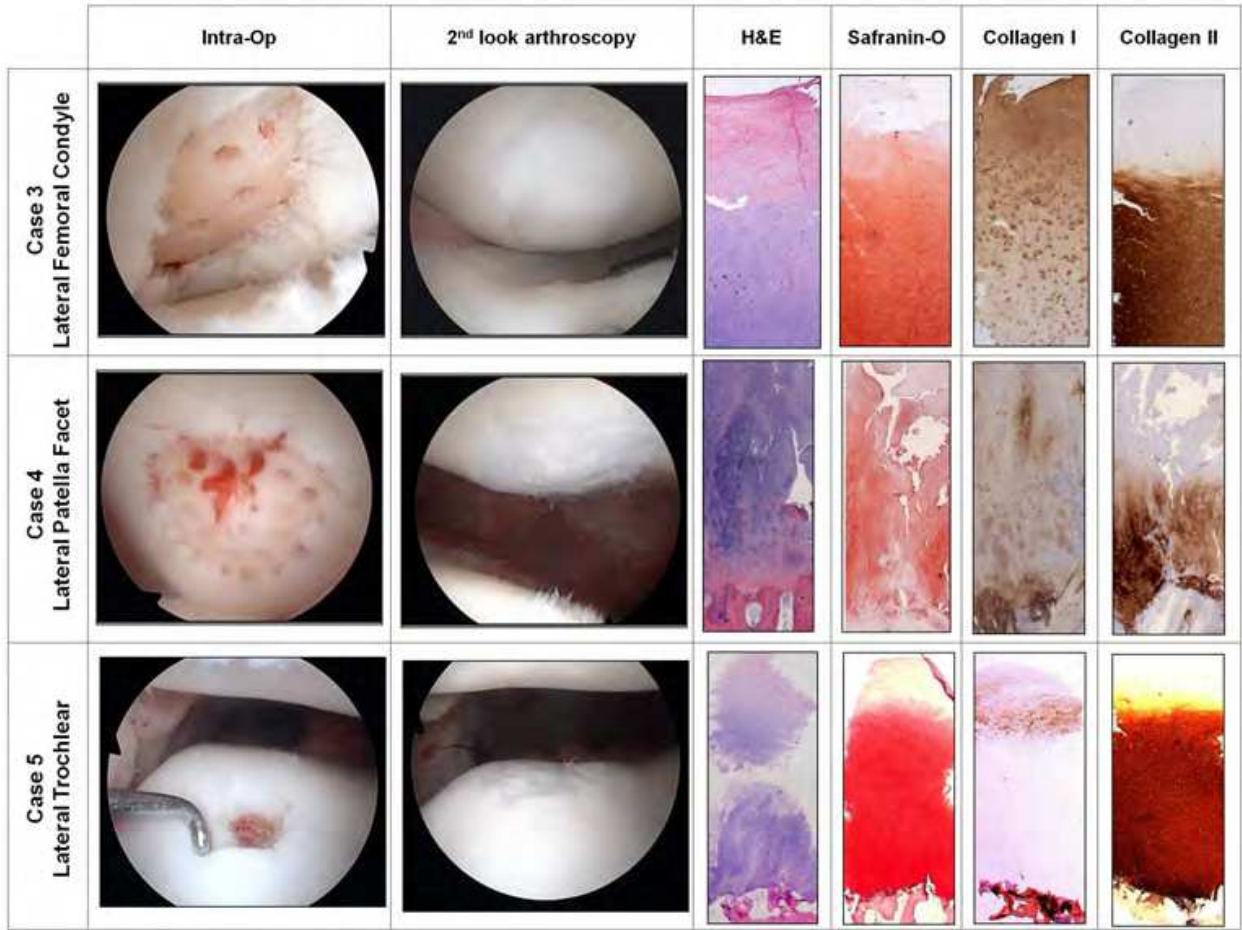


Fig. 23. Second-look arthroscopy and histological images of a lesion from the lateral femoral condyle (Case 3), a lesion from the lateral patella facet (Case 4) and a lesion from the lateral trochlear (Case 5).



### 7.4.3 Chondrogenesis with PBPC and HA

Findings from second-look arthroscopy presented in the above 5 case series confirmed that it was possible to replicate the results of our animal model (Saw et al, 2009) in the human knee joint using a combination of postoperative intraarticular injections of autologous PBPC with HA after arthroscopic subchondral drilling. This method uses marrow stimulation to create an autologous scaffold that is subsequently seeded with both intraarticular injections of autologous PBPC and in-situ progenitor cells from the underlying marrow (Fig 24).

### 7.4.4 Contained lesion

In a typical chondral lesion of the medial femoral condyle (Fig 24) measuring 2cm x 2cm, chondrogenesis progresses as described in Fig 24.

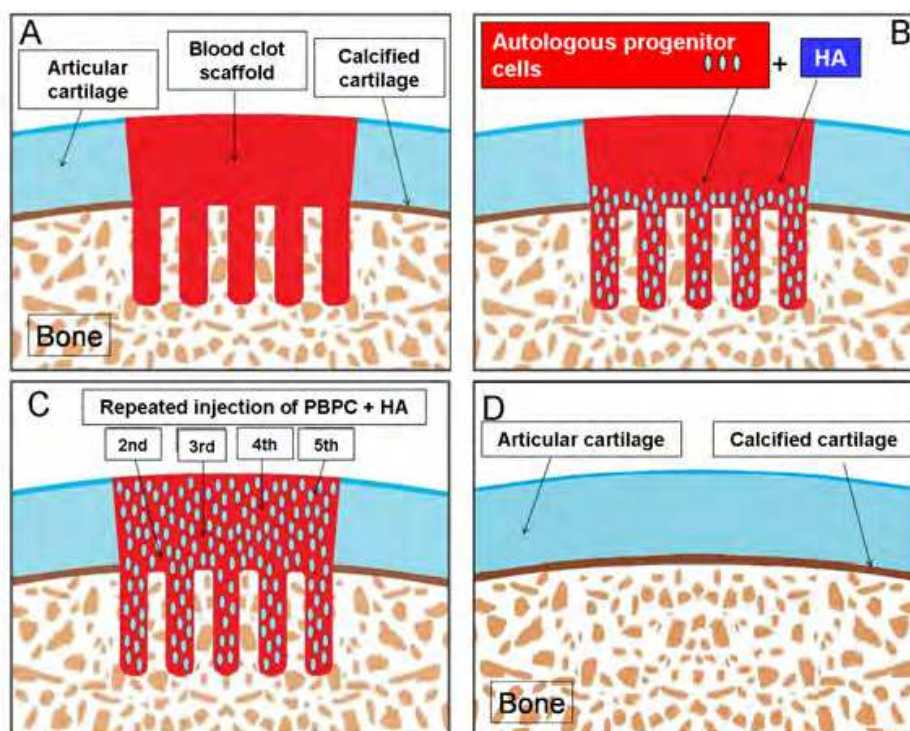


Fig. 24. Chondrogenesis: Contained lesion. (A) A blood clot scaffold is formed after subchondral drilling and abrasion chondroplasty between the drill holes. The surrounding articular cartilage is normal with the underlying calcified cartilage layer and subchondral bone. (B) Injection of fresh PBPC plus HA 1 week after surgery results in the homing of the PBPC into the blood clot scaffold. (C) The PBPC residing in the osteochondral junction and blood clot scaffold gradually transform to chondrocytes. HA helps to reduce inflammation and provide raw material for chondrogenesis. The injected PBPC exert paracrine effects and recruit in-situ progenitor cells to assist in chondrogenesis. Repeated injections of PBPC plus HA enable more cells to be recruited into the chondral defect and enhance chondrogenesis. (D) The final result is the formation of a new layer of articular cartilage with good integration to the surrounding tissues. The ossification of the chondrocytes below the articular cartilage results in repair of the subchondral bone with re-establishment of the calcified cartilage layer.



#### 7.4.5 Uncontained Lesion – Sparse drilling

Second-look arthroscopy in case 2 revealed tufts of cartilage in between areas devoid of regenerated cartilage. The subchondral drilling over the lateral patellofemoral joint was spaced at 3 to 5 mm apart. Fig 25 provides an explanation. As a result, we have refined our techniques so that a goal of 1 to 2 mm between drill holes is now sought. Abrasion chondroplasty up to a depth of 1 mm is also performed.

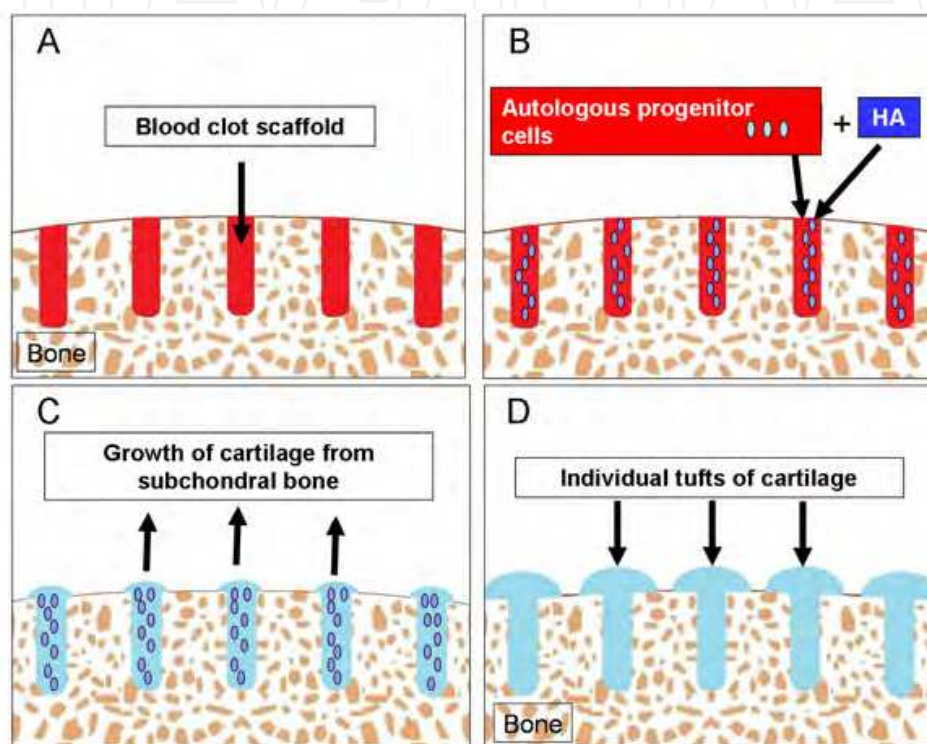


Fig. 25. Chondrogenesis: Uncontained lesion—sparse drilling. (A) In large chondral defects with areas of bare bone, the only available blood clot scaffold is from the areas after subchondral drilling. (B) Injection of fresh autologous PBPC plus HA 1 week after surgery will result in the homing of the PBPC into the subchondral blood clot scaffold, with the PBPC residing in the blood clot scaffold. (C) Because there is no blood clot scaffold superficial to the subchondral bone, chondrogenesis can only be achieved by the protruding tufts of cartilage from the subchondral bone drilling. (D) If the subchondral drill holes are placed too far apart, the end result is the incomplete coverage of the subchondral bone with individual tufts of cartilage seen between areas devoid of cartilage.

#### 7.4.6 Uncontained Lesion – Ideal drilling

Ideally placed drill holes with abrasion chondroplasty allows for a larger surface area and volume of blood clot scaffold to form. When seeded with PBPC and HA, chondrogenesis progresses evenly and the individual tufts of growing cartilage coalesce to form a new layer of articular hyaline cartilage.

Our current method of subchondral drilling in large uncontained lesion is shown in Fig 26.

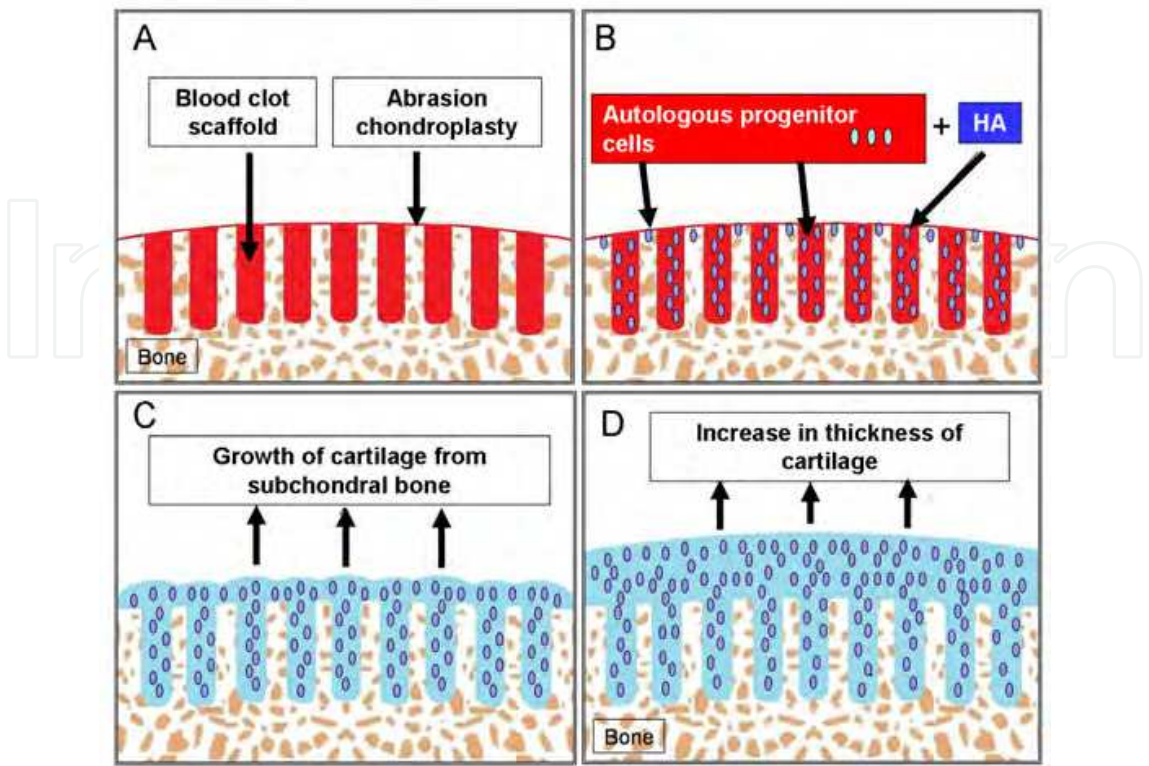


Fig. 26. Chondrogenesis: Uncontained lesion—ideal drilling. (A) Ideally placed subchondral drilling (1 to 2 mm apart) and abrasion chondroplasty between the drill holes increase the available bony areas for the homing of the PBPC. (B) Injected PBPC and HA have a larger surface area of raw bone providing homing signals for the recruitment of the PBPC. (C) Individual tufts of cartilage arise from the subchondral bone and coalesce to cover the bony defect. (D) Maturation will result in an increase in thickness of the regenerated cartilage covering the entire defect.

**7.4.7 Further cases to support the theory of chondrogenesis with ideal drilling in uncontained lesion**

The following cases illustrate the advances made in the light of the histological findings following second-look arthroscopy as regards to the importance of meticulous surgical technique, adjuvant PBPC & HA therapy and cell viability. Chondral lesions in difficult to access region of the knee joint presented a special challenge to treatment. An example would be the posterior aspects of the medial and lateral tibial plateau. In the early phase of the clinical trial, the first author used a technique called the “Inkwell” (Fig 27) procedure in which a 4 mm burr was used to create multiple half moon-shaped pits into the bone surface.

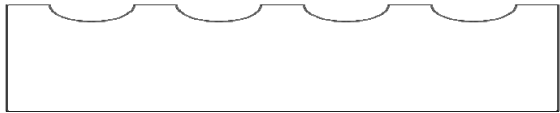


Fig. 27. Illustration of an “Inkwell” procedure.

**Case 6:** A 53-year-old man with a varus knee presented with the loss of the articular cartilage over the medial compartment. He underwent a high tibial osteotomy with the fixation of a Tomofix plate. Postoperative intraarticular injections of PBPC in combination with HA were given in accordance with the standard protocol.

The medial femoral condyle underwent ideal subchondral drilling of the uncontained lesion (Fig 28). In the medial tibial plateau, ideal subchondral drilling was performed over the anterior half of the tibial plateau. Due to poor access, it was not possible to perform subchondral drilling over the posterior half of the tibial plateau. Therefore the “Inkwell” procedure was applied over the posterior half of the tibial plateau (Fig 29).



Fig. 28. The corresponding arthroscopic views over the medial femoral condyle. (A) Intraoperative view and (B) view at 18 months.

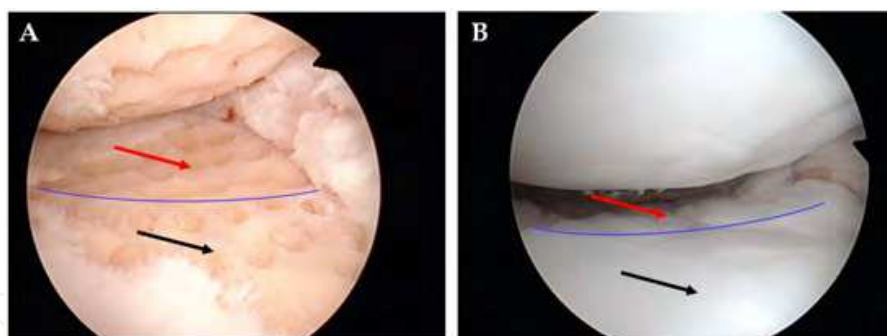


Fig. 29. (A) Arthroscopic view with black arrow showing ideal subchondral drilling over the anterior half of the medial tibial plateau. Red arrow showing the multiple “inkwells” created in the posterior half of the medial tibial plateau. The blue line indicates the border separating the two distinct procedures. (B) Second-look arthroscopy at 18 months showing ideal chondrogenesis in the anterior half of the tibial plateau as compared to the posterior half.

Fig 30 shows the radiological reappearance of the medial articulation at 7 months after surgery. MRI scan at 18 months confirmed the presence of repair cartilage over the anterior half of the medial compartment (Fig 31), confirmed on second-look arthroscopy (Fig 29). This is in contrast with the repair appearance of the posterior half of the tibial plateau (Figs 29 and 32).



Fig 30. A 53-year-old male underwent high tibial osteotomy: (A) Preoperative XR showing narrowing of medial compartment; and (B) Postoperative view at 7 months showing re-appearance of the medial compartment.

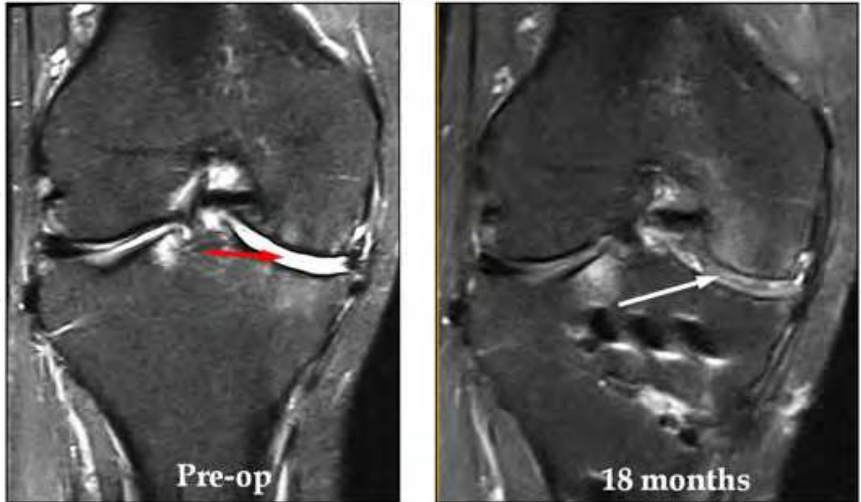


Fig. 31. Preoperative (Pre-op) MRI (STIR) showing 'bone on bone' over the medial compartment of the right knee (red arrow). White arrow showing regenerated articular cartilage at 18 months over the anterior half of both the medial femoral condyle and medial tibial plateau.



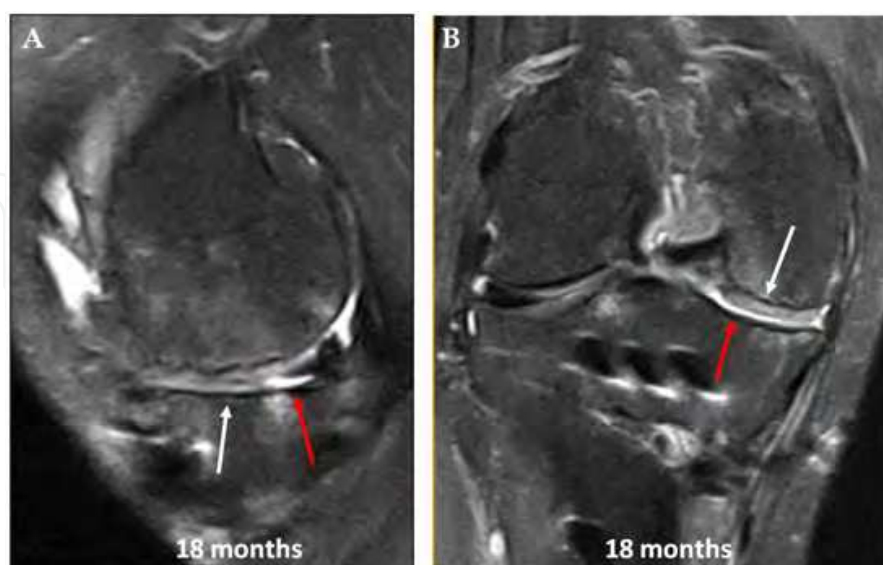


Fig. 32. (A) Sagittal MRI (STIR) over the medial compartment. White arrow over the anterior half of the medial tibial plateau showing evidence of chondrogenesis. Red arrow over the posterior half of the medial tibial plateau whereby the “Inkwell” technique was applied showed minimal chondrogenesis. (B) Coronal MRI (STIR) over the posterior half of the medial tibial plateau. White arrow over the medial femoral condyle showing chondrogenesis. Red arrow over the medial tibial plateau showed minimal chondrogenesis.

Histology from the chondral core biopsy of the medial femoral condyle and anterior half of the medial tibial plateau confirmed the regeneration of hyaline cartilage (Fig 33). This case further supports the theory of ideal drilling with abrasion chondroplasty in uncontained lesions (Figs 26 and 28). With ideally placed drill holes and abrasion chondroplasty, there will be a larger volume of blood-clot scaffold for the injected PBPC and HA to form closely integrated individual tufts of cartilage. These closely seeded tufts arising from the subchondral bone will eventually coalesce to cover the bony defect. Chondrogenesis with maturation will result in increasing thickness of the regenerated cartilage covering the entire defect.

In the absence of subchondral drilling over the posterior half of the medial tibial plateau, the “Inkwell” procedure only produces minimal surface coverage as compared to the anterior half of the tibial plateau.

**Case 7:** A 45-year-old woman underwent right knee arthroscopic lateral patellar release and ideally placed subchondral drilling to the lateral patella facet and lateral trochlear (Fig 34). Beginning one week after surgery, 5 weekly intraarticular injections of HA were given to the operated knee. No PBPC was added to the HA during the intraarticular injections. Radiographs (Fig 35) show improvement of the lateral patellofemoral articulation. In the absence of PBPC in combination with HA, the repair process was only patchy in some areas and the regenerated tissue was found to be of fibrocartilage in nature (Fig 34 and 36).

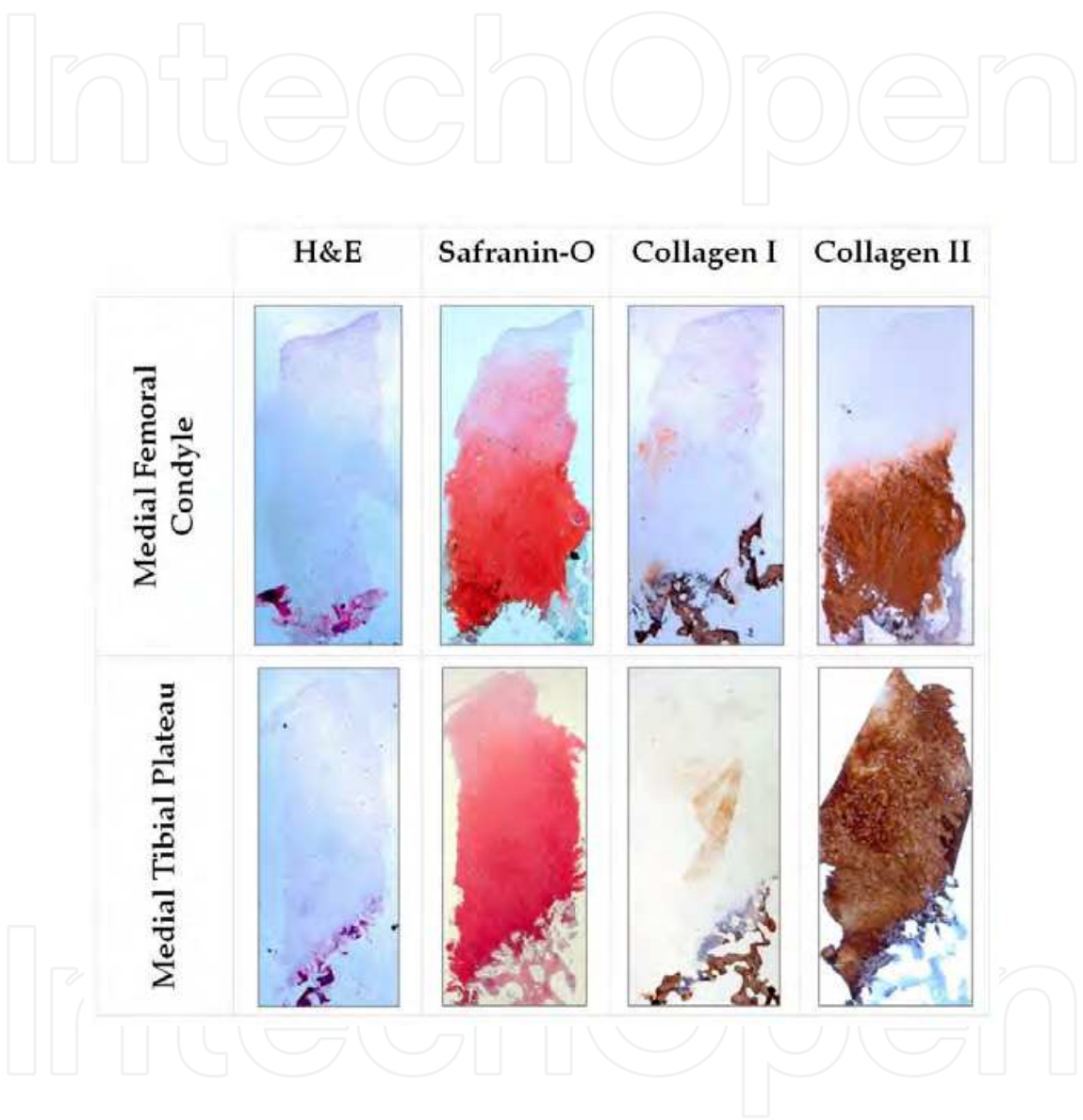


Fig. 33. Case 6 – Histological features showing hyaline cartilage regeneration from the medial femoral condyle and medial tibial plateau biopsies.

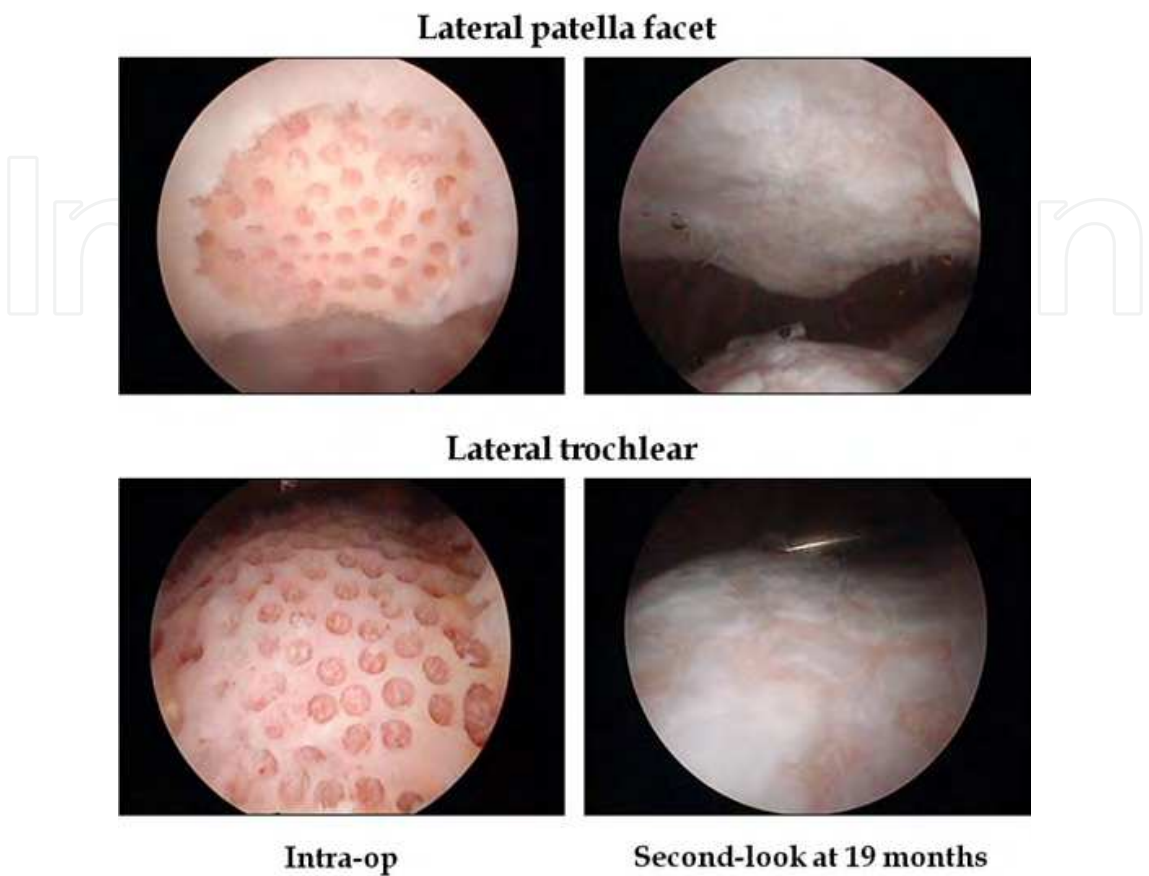


Fig. 34. A 45-year-old woman with intraoperative (Intra-op) and second-look arthroscopy at 19 months. Despite ideal drilling but without postoperative intraarticular injections of PBPC + HA, the end result was only patchy coverage of the bony defects.

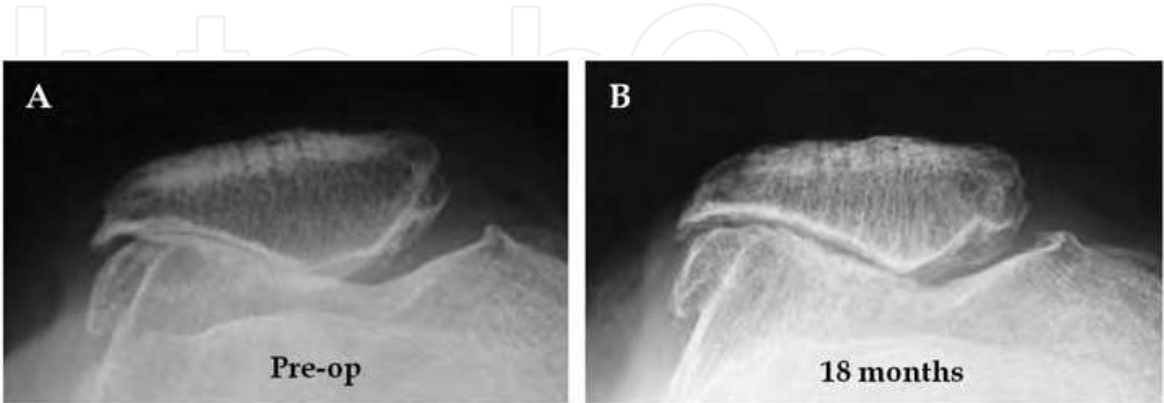


Fig. 35. (A) Preoperative (Pre-op) merchant view showing lateral patellar maltracking with absence of the lateral patellofemoral articulation. (B) XR at 18 months showed improvement of the lateral patellofemoral articulation.

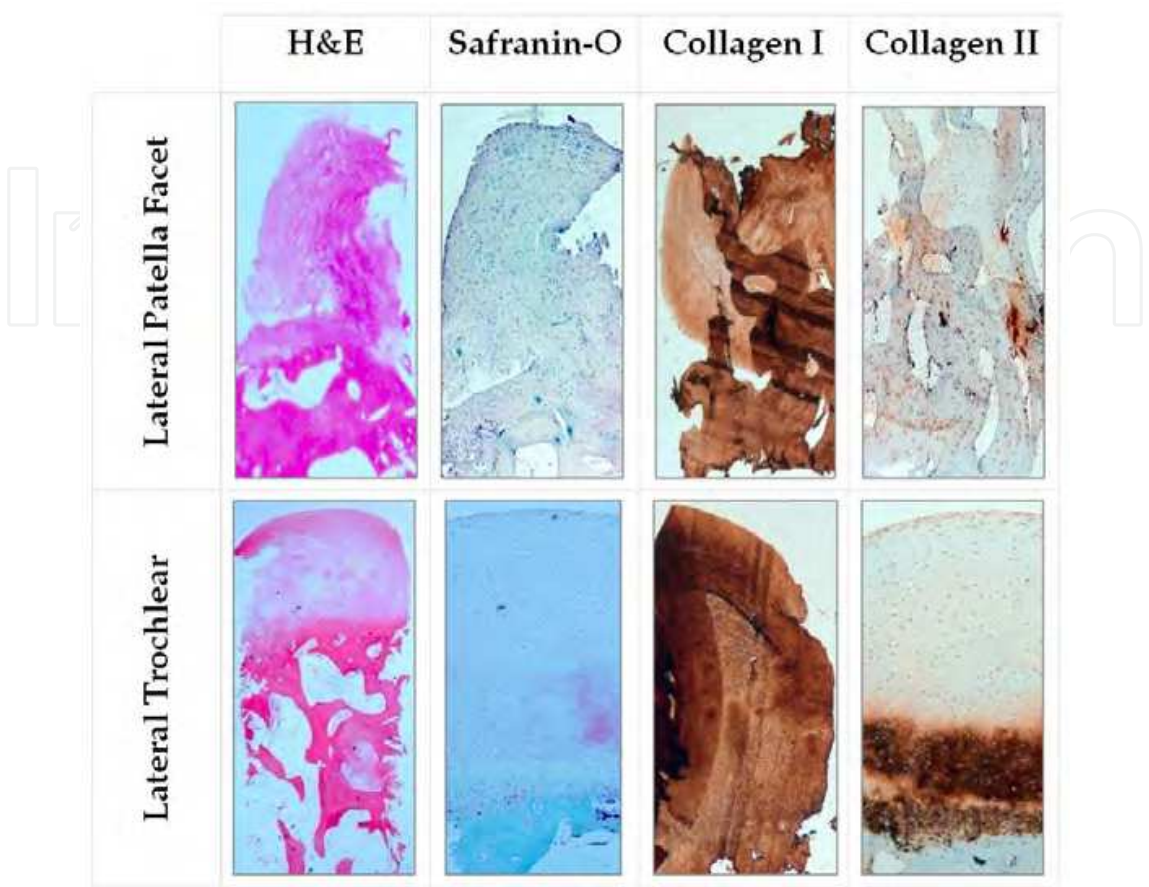


Fig. 36. Case 7 - Histological features showing fibrocartilage repair from the lateral patella facet and lateral trochlear biopsies.

The importance of adjuvant PBPC in combination with HA is well emphasised in this case. In the absence of PBPC, even though ideal subchondral drilling was performed, intraarticular injections of HA alone is ineffective in complete coverage of the bony drill holes and initiate satisfactory articular cartilage repair.

**Case 8:** A 49-year-old man underwent high tibial osteotomy with Tomofix plate fixation, lateral patellar release and ideal subchondral drilling into the tri-compartmental chondral defects. PBPC in combination with HA were injected intraarticularly into the operated knee 1 week after surgery for a total of five weeks. Postoperative radiographs at 19 months showed reappearance of the lateral patella articulation and improvement of the medial compartment (Fig 37).

Second-look arthroscopy with chondral core biopsy from the lateral trochlear (Fig 38), medial and lateral femoral condyles (Fig 39) showed evidence of hyaline cartilage regeneration (Fig 40). In contrast to case 7 which presented with only chondral defects over the lateral patellofemoral joint, case 8 showed satisfactory chondrogenesis with hyaline cartilage regeneration in all 3 compartments. With the addition of postoperative intraarticular injections of PBPC and HA following subchondral drilling, it is possible to address multiple chondral lesions in addition to the difficult to treat “Kissing” lesions.





Fig. 37. A 49-year-old man underwent high tibial osteotomy, lateral patellar release and tri-compartmental chondral drilling.

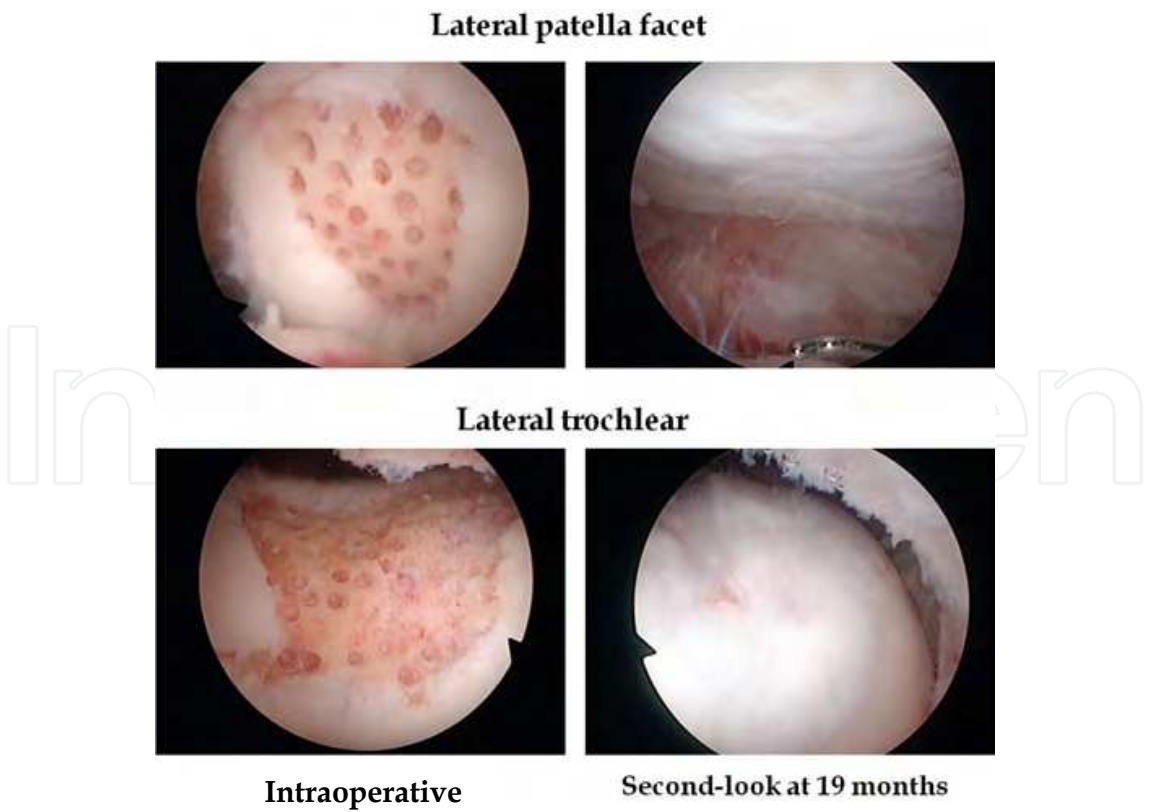


Fig. 38. Second-look at 19 months showed satisfactory coverage of the bony defects by the regenerated tissue.

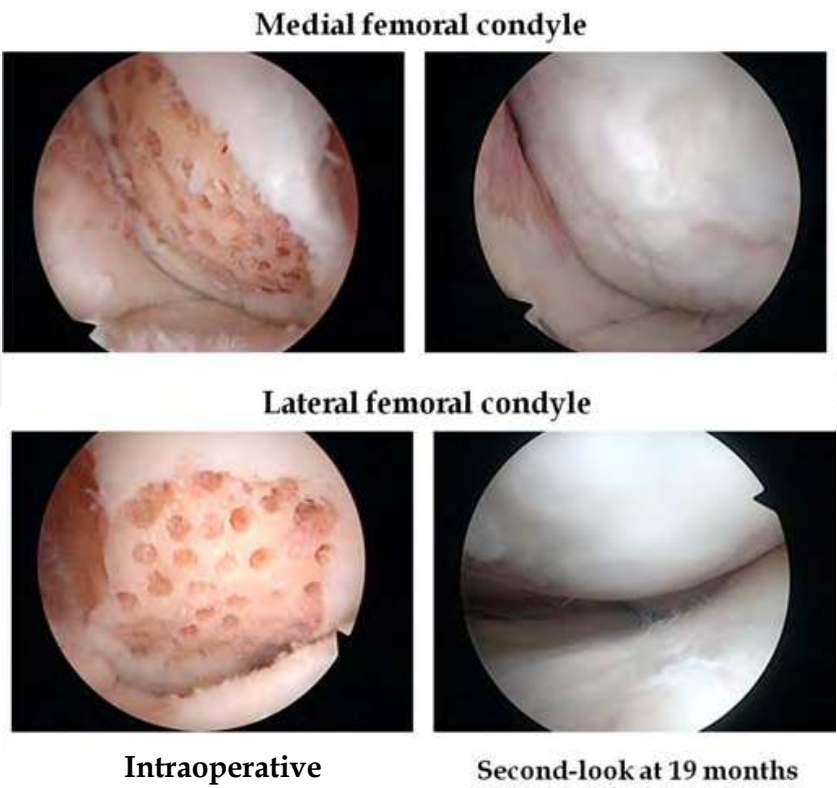


Fig. 39. Second-look at the medial and lateral femoral condyles showed satisfactory chondrogenesis.













	H&E	Safranin-O	Collagen I	Collagen II
Lateral Trochlear (LT)				
Lateral Femoral Condyle (LFC)				
Medial Femoral Condyle (MFC)				

Fig. 40. Case 8 - Histological features showing hyaline cartilage regeneration from the LT, LFC & MFC biopsies.

#### **7.4.8 The importance of PBPC + HA as adjuvant therapy following ideal subchondral drilling**

Case 6 emphasizes on the importance of the improved technique of ideal drilling in an uncontained lesion. Cases 7 & 8 illustrates the importance of postoperative intraarticular injections of PBPC + HA.

Possible reasons as to why the microfracture technique has not been successful in achieving consistent coverage with hyaline cartilage can be explained by what is seen on second-look arthroscopy in cases 6, 7 and 8. Firstly, microfractures are usually placed 3 to 5 mm apart and do not penetrate much deeper than the calcified cartilage layer. Microfractures placed more superficially and further apart as compared to ideal subchondral drilling explains one of the possible reasons why the microfracture technique is inconsistent in producing satisfactory articular cartilage repair. Secondly, like the animal model in Fig 9, without postoperative adjunct therapy with PBPC + HA, the regenerated tissue will always be of inferior quality.

#### **7.4.9 Role of weight-bearing**

Our biopsy specimens from cases with subchondral drilling followed by postoperative intraarticular injections of PBPC in combination with HA showed histologic features of hyaline cartilage with anti-collagen type I stain (used to highlight collagen type I), anti-collagen type II stain (used to highlight collagen type II), and Safranin-O stain (used to highlight proteoglycans), with the exception of one histologic sample showing mixed cartilage. This biopsy specimen was from an area of abrasion notchplasty, which represented a non-weight-bearing region. Comparison of biopsy specimens from this non-weight-bearing area to those from a weight-bearing area in the same patient has led us to theorize that early partial-weight-bearing is essential for the regeneration and alignment of collagen type II (Fig 18).

#### **7.4.10 Articular cartilage imaging of the knee**

Articular cartilage is visible on most standard MRI sequences as a band of intermediate to high signal covering the articular aspect of the bone. Non-injured articular cartilage normally shows a continuous subchondral dark line (low-signal) below the articular cartilage. This dark line likely represents the layer of calcified cartilage and the associated subchondral bone plate. It may be accentuated by chemical shift artifact (of water and fat molecules in the same voxel canceling their respective signals thereby resulting in signal loss). Fig 41 illustrates the articular cartilage and subchondral bone on a sagittal PD image. Evaluating postoperative MRIs, we assessed the restoration of the dark line as evidence of calcified cartilage with subchondral bone healing and fill of the defect as indicative of cartilage regeneration.

Our current imaging preference for assessing chondral lesions of the knee joint utilize 2D PD and PDFS sequences using a high field (1.5T) extremity MRI (GE Medical Systems) – Fig 42. This has the benefits of improved signal to noise and higher resolution. Fig 43 showing examples of chondral lesions seen following MRI scan with arthroscopic correlation (Fig 44). Our earlier cartilage images were obtained by an open MRI system operating at 0.35T (Magnetom C!, Siemens Medical Solutions, Erlangen, Germany) using an extremity receive coil.

MRI scans were utilized preoperatively as part of the diagnostic work up and postoperatively to monitor healing of the chondral defects. We performed MRI scans at

shorter intervals for our first 10 patients. Scans were performed on the first postoperative day as a baseline to document the chondral defect after debridement and subchondral drilling. Serial studies were then collected in the postoperative period (at 6, 12, 18, 24 months and beyond) to evaluate the filling of the defect by regenerated cartilage and changes in the subchondral bone.

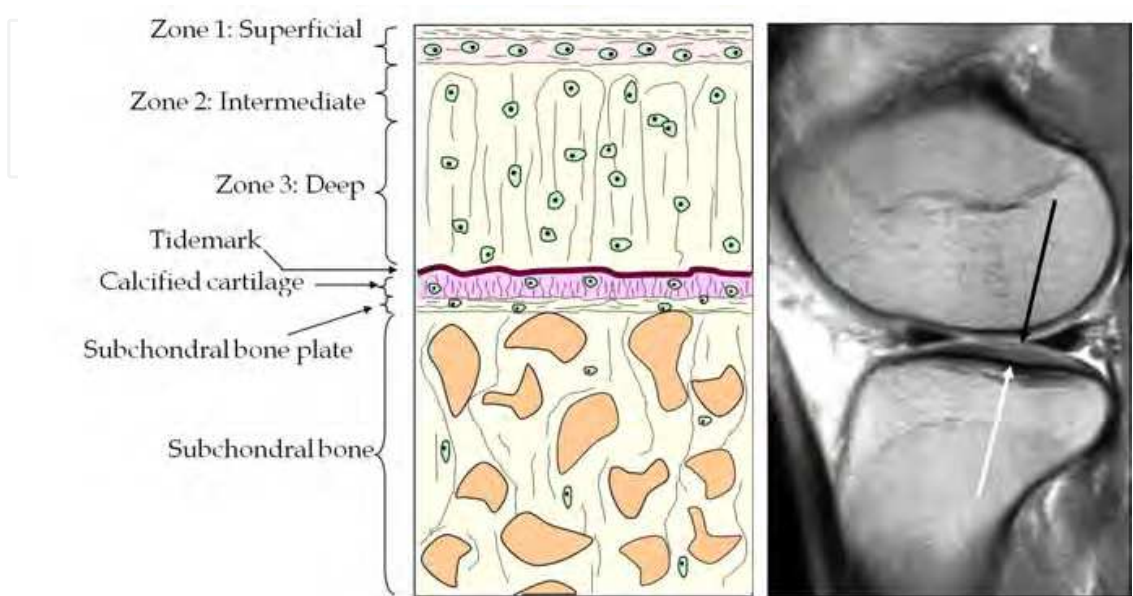


Fig. 41. Articular cartilage as depicted by sagittal PD image at the tibial plateau. Black arrow showing the surface of the tibial plateau articular cartilage and red arrow showing the “Black line” that separates the articular cartilage from the subchondral bone. This layer correlates with the tidemark / calcified cartilage / subchondral bone plate layers.



Fig. 42. A patient with her right knee in a high field extremity (1.5T) MRI (GE Medical Systems).



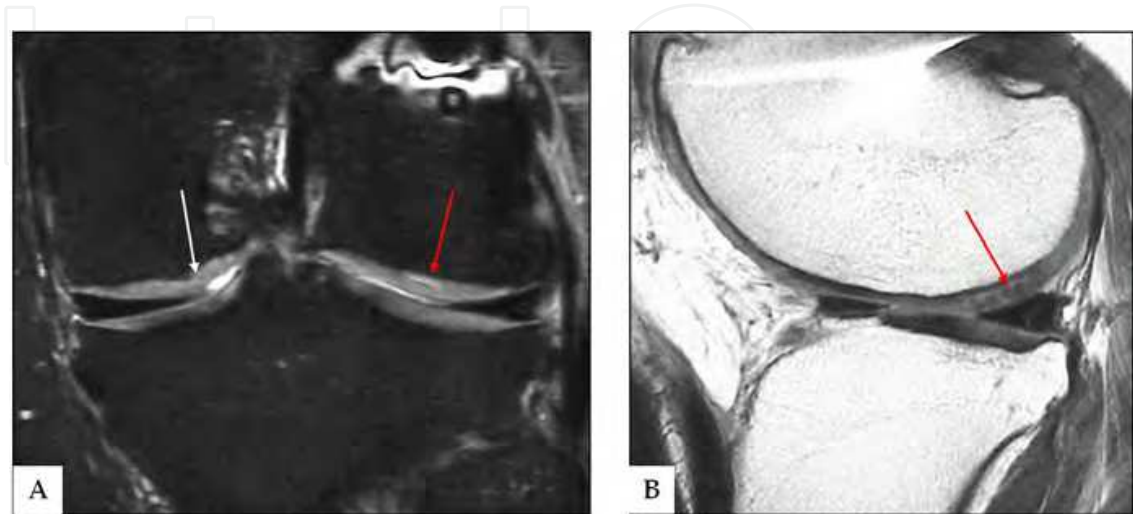


Fig. 43. Images of chondral lesions demonstrated by extremity high field MRI at 1.5T. (A) Chondral flap tear of the medial femoral condyle (white arrow) with red arrow showing a delaminated chondral lesion over the lateral femoral condyle (PDFS). (B) The corresponding chondral lesion of the lateral femoral condyle (red arrow) on a sagittal PD image.



Fig. 44. Corresponding arthroscopic view of the lesions from the medial femoral condyle (MFC) and lateral femoral condyle (LFC) as in Fig 43.

MRI scans performed on the first postoperative day showed the chondral defects as well delineated from surrounding healthy cartilage. The chondral defects were bare or partially filled in with blood clot. Drill tracts and subchondral marrow edema were clearly observed (Figures 45 to 47). Subchondral bone is disrupted, i.e. there is loss of the continuity of the subchondral black line. Over the course of two years, filling-in of the chondral defects by material of similar or same signal as articular cartilage was observed. Re-establishment of subchondral black line paralleled the progressive resolution of marrow edema.

Serial MRI scans of our first patient undergoing this treatment are presented in Figure 45. After full debridement and drilling, the chondral defect is well visualized as a bare area partially filled by clot (Figure 45A). The low signal subchondral bone is disrupted and low signal drill tracts are visualized within the subchondral marrow edema. The disruption of the subchondral dark line represents a conduit through the calcified cartilage layer. Serial scans showed progressive filling of chondral defects by material of similar appearance as articular cartilage, resolution of marrow edema and reappearance of the continuous subchondral dark line (Figure 45B). At one to two years, the calcified cartilage, as depicted by the low signal band, becomes almost as thick at the site of drilling as in the surrounding healthy areas. (Figure 45D). Figures 46 and 47 present an additional patient.

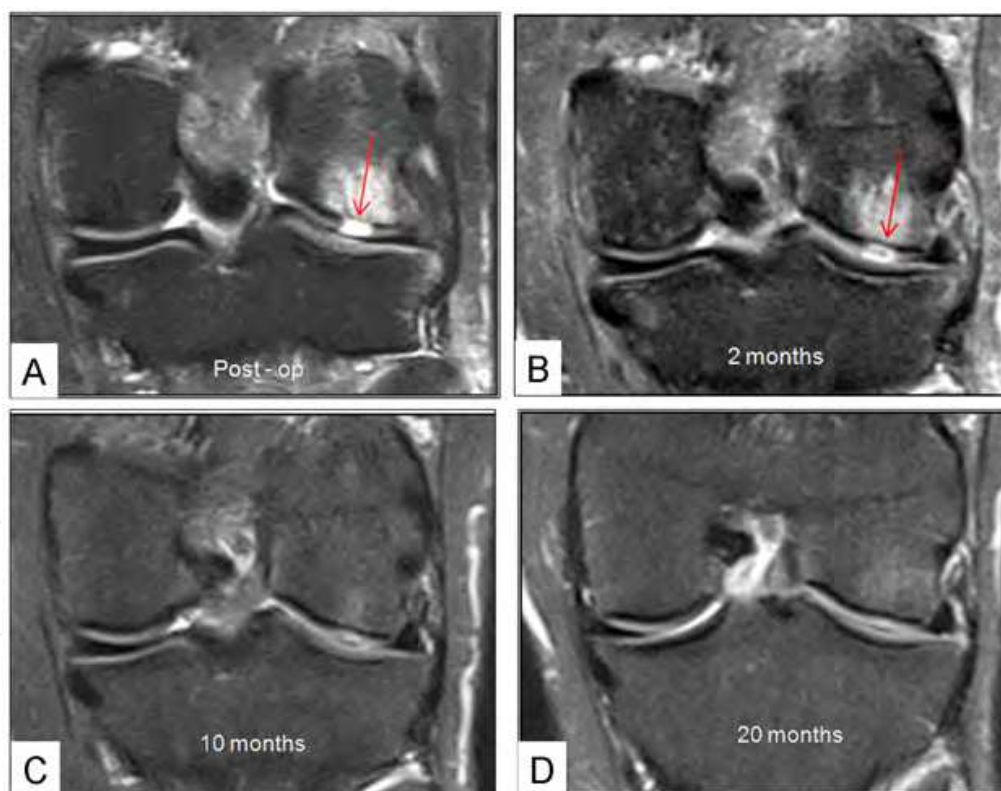


Fig. 45. Serial MRI evaluation (STIR images at 0.35T). Postoperative (Post-op): note the disruption of the subchondral dark line (red arrow). (B) 2 months: partial resolution of marrow edema and reappearance of the continuous subchondral dark line (red arrow). (C) 10 months: almost complete resolution of marrow edema and filling of defect. (D) 20 months: complete healing of defect and re-establishment of subchondral dark line representing healing of the calcified cartilage layer.

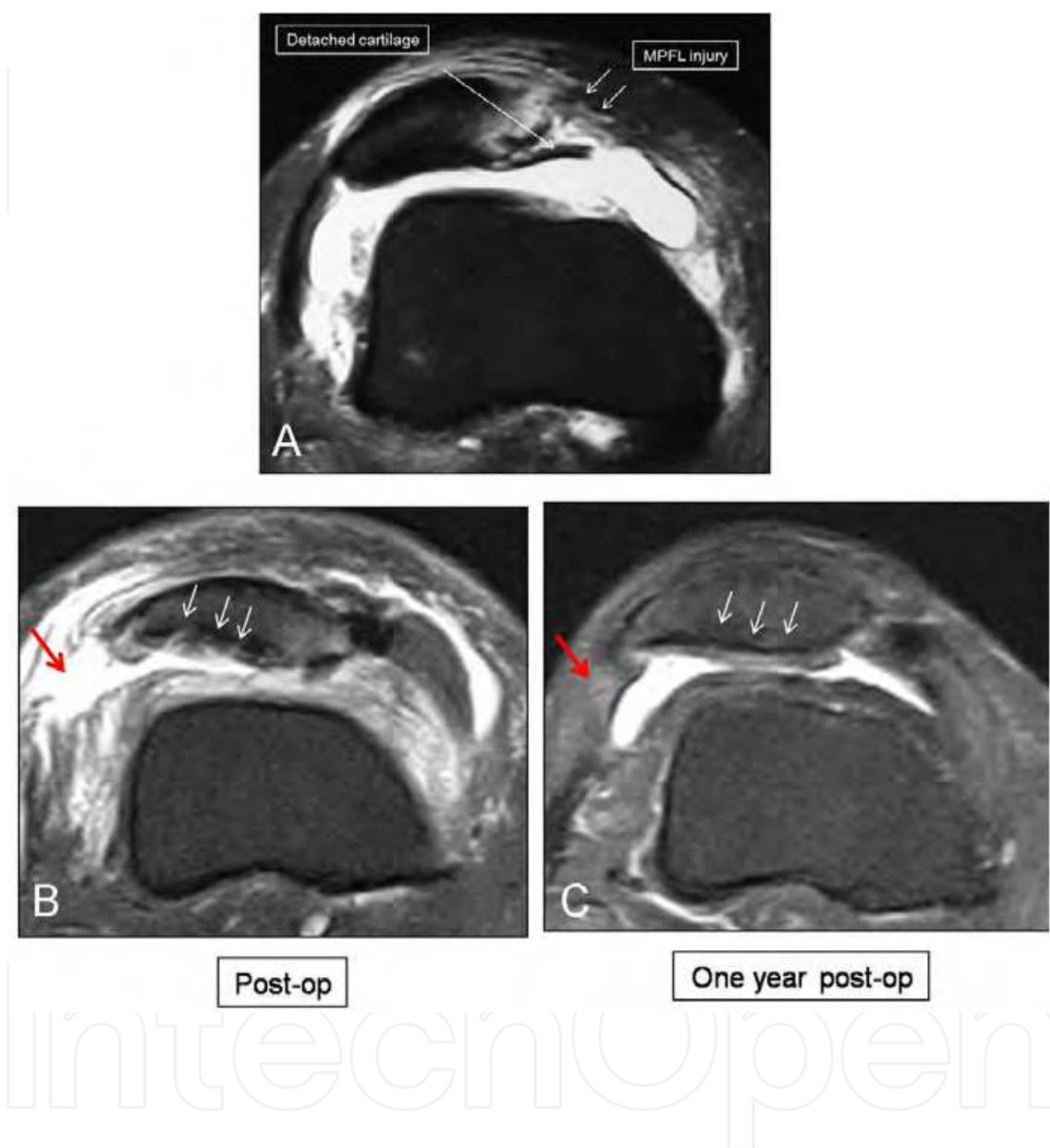


Fig. 46. A 40-year-old woman with patellar dislocation (STIR images at 0.35T). (A) Preoperative MRI with evidence of a delaminating articular cartilage injury and medial patellar femoral ligament (MPFL) injury. The injury was treated with arthroscopic lateral release, subchondral drilling and repair of the MPFL. (B) Postoperative (Post-op) MRI following arthroscopic lateral patellar release (red arrow) and subchondral drilling showing interruption of the low signal subchondral calcified cartilage (white arrows). (C) At one year following surgery, MRI revealed a healed lateral retinaculum (red arrow), re-establishment of the subchondral calcified cartilage (white arrows) and evidence of articular cartilage regeneration at the lateral patella facet.

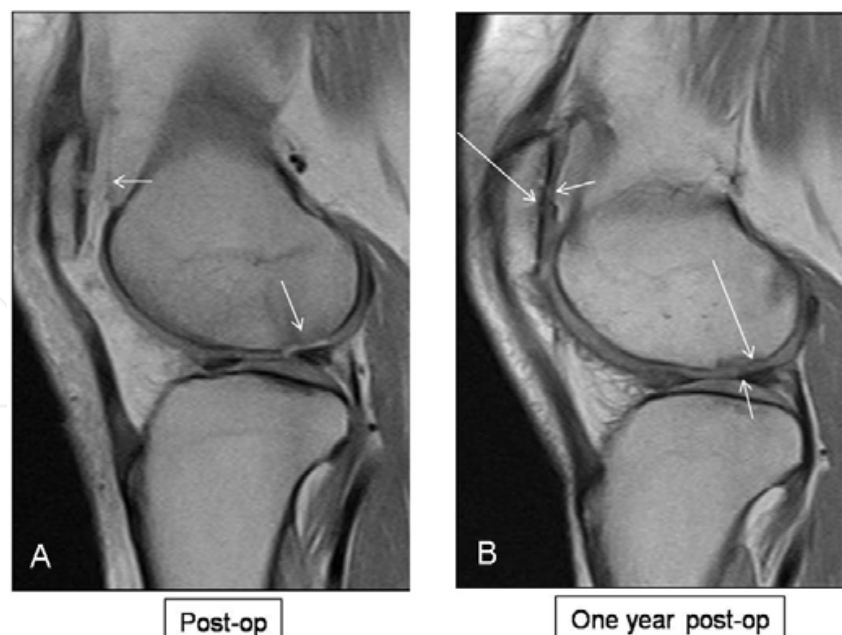


Fig. 47. Sagittal PD MRI (0.35T) of patient in Figure 46. (A) Postoperative (Post-op) MRI: chondral lesions at the lateral patella and lateral femoral chondyle (arrows). Note the disruption to the continuous low signal calcified cartilage layer at both sites. (B) MRI at one year after surgery showing the re-establishment of the subchondral calcified cartilage layer (long arrows) together with articular cartilage regeneration (short arrows).

The re-establishment of the calcified cartilage layer and healing of the subchondral bone are important MRI features of articular cartilage regeneration in our series. This is accompanied by filling of the chondral defect. Following arthroscopic subchondral drilling, MRI images revealed extensive marrow edema and interruption of the calcified cartilage layer together with the underlying subchondral bone. This is shown as disruption of the low signal subchondral dark line. As the injected PBPC seed the blood clot scaffold in the presence of HA, chondrogenesis is initiated with the formation of chondrocytes which then occupy the drill holes. This process is gradually replaced by bone resulting in subchondral bone repair. Gradual resolution of marrow edema is observed. The subchondral dark line progressively re-appears on MRI scans indicating the re-establishment of the calcified cartilage layer and healing of the subchondral bone (Figures 45 to 47). This evidence is provided from the histology shown on Figures 20 and 21. Depending on whether the lesion is a contained or uncontained lesion, chondrogenesis follows the gradual re-appearance of this subchondral dark line on serial MRI scans (Figures 24 and 26).

#### 7.4.11 Phase I study clinical outcomes

Since starting clinical trials in 2007, 223 cartilage regeneration cases have been performed on 205 patients. Cases were varied including 38 cases involving isolated cartilage lesions, 92 cases involving multiple cartilage lesions, 54 cases involving patellofemoral cartilage lesions, 7 cases involving concomitant lower limb realignment procedures, and 32 cases involving ligament reconstruction. When evaluating two-year clinical outcomes, 24 months has passed for 155 of these 223 cases. Within this group, 52 cases have preoperative, 12-month, and 24-month IKDC values available for clinical outcome evaluation. This group had a preoperative IKDC average of 50.5, a 12-month IKDC



average of 70, and a 24-month IKDC average of 70. 30 patients had 30-month data available and illustrated a 30-month IKDC average of 71 (Fig 48).

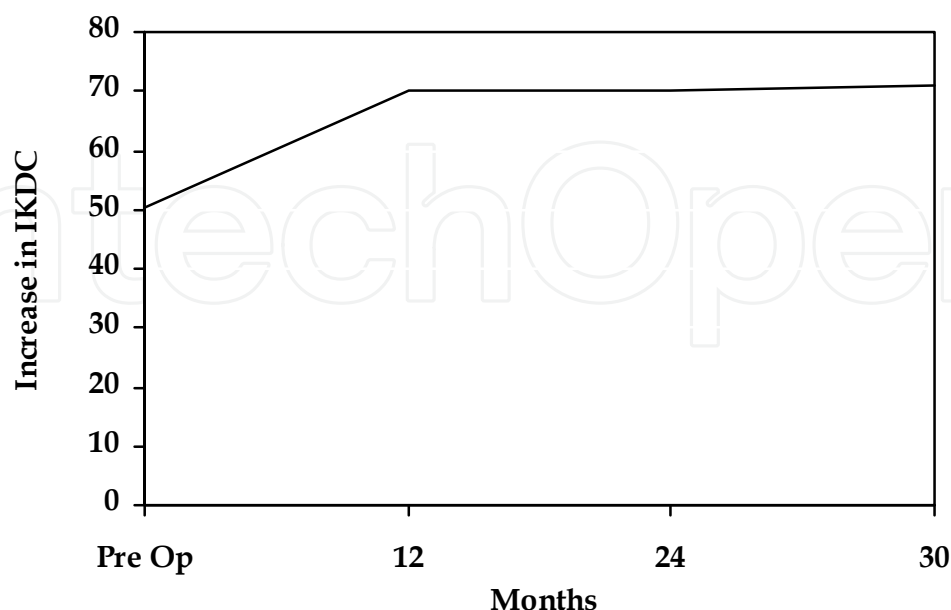


Fig. 48. International Knee Documentation Committee (IKDC) outcomes.

Our IKDC results illustrated a significant increase similar to studies documenting overall outcomes in the literature with marrow stimulation and chondrocyte implantation. Historically, microfracture has shown a peak functional outcome at 24 months (Blevins et al, 1998; Peterson et al, 2000; Steadman et al, 2003; Gobbi et al, 2005; Mithoefer et al, 2005; Knutsen et al, 2007). Two studies have illustrated a decline after the first 18 to 24 months with microfracture, including Mithoefer et al (2005) documenting 69% of their patients reporting lower IKDC scores after 24 months. Conversely, two outcome studies have found sustained improvement at the 24-month time interval (Steadman et al, 2003; Knutsen et al, 2004). In comparison of these four studies, the average age of the study groups documenting decline was 39.5 years and 41 years. In contrast, the average age of the studies documenting sustained improvement was 30.4 years and 31.1 years (Steadman et al, 2003; Mithoefer et al, 2005; Kruez et al, 2006; Knutsen et al, 2004). In a group with an average age of 47.1 years, our IKDC scores showed sustained improvement at 24 months with 30 cases documenting continued improvement at 30 months.

Comparing microfracture and chondrocyte implantation, decisive superiority has not been established. Two randomized studies have sought to directly compare outcomes with differing results. Saris et al. (2009) found significantly better outcomes with ACI at 36 months. They found a continued increase in Knee Injury and Osteoarthritis Outcome Scores (KOOS) from 6 to 36 months with ACI and a plateau in scores at 18 months with microfracture (Saris et al, 2009). However, Knutsen et al. found no significant clinical or radiographic difference between microfracture and ACI at 60 months utilizing four clinical outcome scoring systems and 2 radiologic outcome systems (Knutsen et al, 2007). Zeifang et al. (2010) in comparison of conventional methods of ACI with refined methods of ACI for treatment of femoral chondral lesions found an increase from a baseline IKDC (51.1) by 21 points and 25 points respectively. This series had an average age of 29.3 years (Zeifang et al, 2010). At 24 months, this rise declined slightly in the conventional method to 19 points

above baseline and remained stable in the refined method at 25 points above baseline (Zeifang et al, 2010). This compares to our rise above a baseline IKDC of 50.5 by 20 points at 12 months, 20 points at 24 months, and 21 points at 30 months (Fig 48). Of note, our patient group has a mean age of 47.1 years and included patients with multiple chondral lesions, while Zeifang et al. (2010) evaluated isolated defects of the femoral condyle.

Our clinical results indicate that the regenerated tissue is resilient and coincide with histological results suggesting that this technique produces hyaline cartilage. However, evaluating phase I data has weaknesses. As this portion of the clinical trial has included evolution in technique and cell processing, there is some inherent variation. Additionally, IKDC collection was inconsistent in the initial phases. Also, when attempting to evaluate this early data, there is no control group available for comparison. Currently a randomized controlled trial is underway under the direction of the first author.

#### **7.4.12 Complications**

Specific complications are mild bone pain associated with Neupogen injections, and discomfort of PBSC harvesting and localized pain following intraarticular injections with PBPC and HA. One male patient in his mid-forties had a previous infection from Anterior Cruciate Ligament (ACL) surgery, multiple microfractures and subsequent ACL revision surgery with postoperative PBPC and HA. He had recurrence of intercondylar osteophytes and reactive arthritis and eventually chose a total knee replacement. Three other patients had secondary procedure for persistent osteophytes and treatment for further areas of chondral degeneration.

It is evident that with adjuvant PBPC and HA therapy, chondrogenesis is possible with hyaline cartilage, but a small proportion of patients may return for further treatment because of newly diagnosed areas of chondral degeneration in the treated knee.

#### **7.5 Current control randomized trial**

A randomized controlled trial comparing a group with PBPC and HA injections with a group with HA injection alone following arthroscopic subchondral drilling is currently under way, being supervised by the first author. The early results seem to support the benefit of adjuvant postoperative intraarticular injections of PBPC in combination with HA.

#### **7.6 Summary of theory**

Our theory is that providing a high percentage of immature multipotent progenitor cells into the right environment allows these cells to populate areas of subchondral drilling and regenerate hyaline cartilage. Our histologic findings of chondrocytes below the calcified cartilage layer at a subchondral drill hole (Figs 20 and 21) and the porcine model (Lee et al, 2007) illustrating mesenchymal stem cells at the base of newly formed cartilage support the idea that injected progenitor cells are attracted to the site of marrow injury, proliferate into chondrocytes, and regenerate hyaline cartilage from the subchondral base. We theorize that the addition of matrix substance, in the form of HA and passive stimulating kinetic movement of the involved joint (continuous passive motion), provides chemical and cellular signals for regeneration. Partial to full weight-bearing in the early phase of rehabilitation provides the essential environment to assist in the remodelling of the collagen fibrils to align along the axis of weight transmission.

## 8. Conclusion

It is evident that for ideal chondrogenesis with hyaline cartilage in contained or uncontained lesions, the correct surgical technique with attention to detail, a postoperative adjuvant therapy with a high percentage of viable PBPC in combination with HA, and the importance of a postoperative rehabilitation program are important. Failure to adhere to these three important basic principles will result in inferior repair tissue which will inevitably deteriorate with time.

Articular hyaline cartilage regeneration is possible with arthroscopic subchondral drilling followed by postoperative intraarticular injections of autologous PBPC in combination with HA.

## 9. References

- Asik, M.; Ciftci, F.; Sen, C.; Erdil, M.; and Atalar, A. (2008). The microfracture technique for the treatment of full-thickness articular cartilage lesions of the knee: midterm results. *Arthroscopy*, Vol 24, No 11, pp 1214-20.
- Blevins FT, Steadman JR, Rodrigo JJ, Silliman. (1998). Treatment of articular cartilage defects in athletes: an analysis of functional outcome and lesion appearance. *Orthopedic*, Vol 21, No 7, pp:761-768.
- Brittberg M, Aglietti P, Gambardella R, et al. (2000). The ICRS clinical cartilage injury evaluation system-2000. *Presented at the 3<sup>rd</sup> Meeting of the International Cartilage Repair Society, Goteborg, Sweden, 2000, April 27-28.*
- Cesselli D, Beltrami AP, Rigo S, et al. (2009) Multipotent progenitor cells are present in human peripheral blood. *Circulation Research* . Vol 104, No 10, pp1225-34.
- Chen et al (2006). Mesenchymal stem cells in immunoregulation. *Immunology Cell Biology*. Vol 84, pp413-421.
- Chung C.A., T.W. Yang, Chen C.W. (2006). Analysis of cell growth and diffusion in a scaffold for cartilage tissue engineering *Biotechnol. Bioeng.* Vol94, No6, pp1138-1146
- Dominici M., K.Le Blanc, I. Mueller, I. Slaper-Cortenbach, F.C. Marini, D.S. Krause, R.J. Deans, A. Keating, D.J. Prockop and E.M. Horwitz (2006). Position Paper: Minimal criteria for defining multipotent mesenchymal stromal cells. The International Society for Cellular Therapy position statement. *Cytotherapy*. Vol8, No 4, pp315 317.
- Flanigan, D. C.; Harris, J. D.; Trinh, T. Q.; Siston, R. A.; and Brophy, R. H. (2010). Prevalence of chondral defects in athletes' knees: a systematic review. *Med Sci Sports Exerc*, Vol42, No10, pp1795-801.
- Fortier, L. A., Potter, H.g., Rickey, E.J., Schnabel, L.V., Foo, L.F., Chong, L.R., Stokol, T., Cheetham, J., and Nixon, A.J., (2010) Concentrated bone marrow aspirate improves full-thickness cartilage repair compared with microfracture in the equine model. *Journal of Bone Joint Surgery America*. Vol92, No 10, pp1927-1937.
- Freedman, K. B.; Fox, J. A.; and Cole, B. J. (2004) Knee Cartilage: Diagnosis and Decision Making. In *Textbook of Arthroscopy*. Edited by Miller, M., and Cole, B., Philadelphia, PA, Eslevier, 2004.
- Gill, T. J. (2000) The treatment of articular cartilage defects using microfracture and debridement. *Am J Knee Surg*, Vol13, No1, pp33-40.

- Gobbi A, Nunag P, Malinowski K. (2005). Treatment of full thickness chondral lesions of the knee with microfracture in a group of athletes. *Knee Surg Sports Traumatology Arthroscopy*. Vol 13, No 3, pp213-215.
- Gooding, C. R.; Bartlett, W.; Bentley, G.; Skinner, J. A.; Carrington, R.; and Flanagan, A. (2006) A prospective, randomised study comparing two techniques of autologous chondrocyte implantation for osteochondral defects in the knee: Periosteum covered versus type I/III collagen covered. *Knee*, Vol13, No3, pp203-10.
- Holig K, Kramer M, Kroschinsky F, et al. (2009) Safety and efficacy of hematopoietic stem cell collection from mobilized peripheral blood in unrelated volunteers: 12 years of single-center experience in 3928 donors. *Blood*. Vol114, No18, pp3757-63.
- Horvai, A. (2011) Anatomy and Histology of Cartilage. In *Cartilage Imaging*. Edited by Link, T., NY, Springer, 2011.
- Jakobsen, R. B.; Engebretsen, L.; and Slauterbeck, J. R. (2005) An analysis of the quality of cartilage repair studies. *J Bone Joint Surg Am*, Vol87, No10, pp 2232-9.
- Johnson, L. L. (1986) Arthroscopic abrasion arthroplasty historical and pathologic perspective: present status. *Arthroscopy*, Vol2, No1, pp 54-69.
- Kang, S. W.; Bada, L. P.; Kang, C. S.; Lee, J. S.; Kim, C. H.; Park, J. H.; and Kim, B. S. (2008) Articular cartilage regeneration with microfracture and hyaluronic acid. *Biotechnol Lett*, Vol30, No3, pp 435-9, 2008.
- Kaplan, L. D. et al. (2009) The effect of early hyaluronic acid delivery on the development of an acute articular cartilage lesion in a sheep model. *Am J Sports Med*, Vol37, No12, pp 2323-7, 2009.
- Knutsen G, Engebretsen L, Ludvigsen TC, et al. (2004). Autologous chondrocyte implantation compared with microfracture in the knee. A randomized trial. *Journal of Bone and Joint Surgery (American)*. Vol 86-A, No 3, pp:455-464.
- Knutsen G, Drogset JO, Engebretsen L, et al. (2007) A randomized trial comparing autologous chondrocyte implantation with microfracture. Findings at five years. *Journal of Bone and Joint Surgery (American)*. Vol 89, No 10, pp:2105-2112
- Koch TG, Berg LC, Betts DH.(2008) Concepts for the clinical use of stem cells in equine medicine. *Can Vet J*. Vol49, No10, Oct 2008, pp1009-17.
- Kreuz PC, Steinwachs MR, Erggelet C, et al. (2006). Results after microfracture of full-thickness chondral defects in different compartments in the knee. *Osteoarthritis Cartilage*. Vol 14, No 11, pp: 1119-1125.
- Kujawa, M. J., and Caplan, A. I. (1986) Hyaluronic acid bonded to cell-culture surfaces stimulates chondrogenesis in stage 24 limb mesenchyme cell cultures. *Dev Biol*, Vol114, No2, pp504-18.
- Kuroda R et al (2007). Treatment of a full-thickness articular cartilage defect in the femoral condyle of an athlete with autologous bone marrow stromal cells. *Osteoarthritis Cartilage*. Vol15, pp226-231.
- Lee, K. B.; Hui, J. H.; Song, I. C.; Ardany, L.; and Lee, E. H.(2007) Injectable mesenchymal stem cell therapy for large cartilage defects--a porcine model. *Stem Cells*, Vol25, No11, pp2964-71.
- Legovic, D. et al. (2009) Microfracture technique in combination with intraarticular hyaluronic acid injection in articular cartilage defect regeneration in rabbit model. *Coll Antropol*, Vol33, No2, pp619-23.

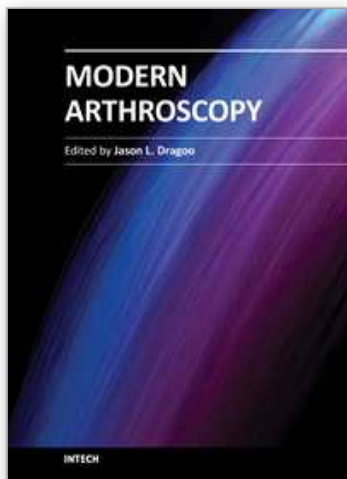


- Lubowitz, J. H.; Appleby, D.; Centeno, J. M.; Woolf, S. K.; and Reid, J. B., 3<sup>rd</sup> (2007) The relationship between the outcome of studies of autologous chondrocyte implantation and the presence of commercial funding. *Am J Sports Med*, Vol35, No11, pp1809-16.
- Magnussen, R. A.; Dunn, W. R.; Carey, J. L.; and Spindler, K. P. (2008) Treatment of focal articular cartilage defects in the knee: a systematic review. *Clin Orthop Relat Res*, Vol466, No4, pp952-62.
- Mankin, H. J.; Mow, V. C.; Buckwalter, J. A.; Iannotti, J. P.; and Ratcliffe, (2000) A.: Articular Cartilage Structure, Composition, and Function. In *Orthopaedic Basic Science 2nd Edition*. Edited by Buckwalter, J. A.; Einhorn, T. A.; and Simon, S. R., AAOS, 2000.
- McCarty R.C., C.J. Xian, S. Gronthos, A.C.W. Zannettino and B.K. Foster (2010). Application of autologous bone marrow derived mesenchymal stem cells to an ovine model of growth plate cartilage injury. *The Open Orthopaedics Journal*, Vol4, pp204-210.
- McGuire, D. A.; Carter, T. R.; and Shelton, W. R. (2002) Complex knee reconstruction: osteotomies, ligament reconstruction, transplants, and cartilage treatment options. *Arthroscopy*, Vol18, No9 Suppl 2, pp 90-103.
- Menche, D. S.; Frenkel, S. R.; Blair, B.; Watnik, N. F.; Toolan, B. C.; Yaghoubian, R. S.; and Pitman, M. I.(1992): A comparison of abrasion burr arthroplasty and subchondral drilling in the treatment of full-thickness cartilage lesions in the rabbit. *Arthroscopy*, Vol12, No3, pp280-6.
- Messner, K., and Maletius, W. (1996) The long-term prognosis for severe damage to weight-bearing cartilage in the knee: a 14-year clinical and radiographic follow-up in 28 young athletes. *Acta Orthop Scand*, Vol67, No2, pp165-8.
- Mithoefer K, Williams RJ 3rd, Warren RF, et al. (2005) The microfracture technique for the treatment of articular cartilage lesions in the knee. A prospective cohort study. *Journal of Bone and Joint Surgery (American)*. Vol 87, No 9, pp: 1911-1920.
- Murphy et al (2003). Stem cell therapy in a caprine model of osteoarthritis. *Arthritis Rheumatology*. Vol48, pp3464-3474.
- Nakamura, N.; Miyama, T.; Engebretsen, L.; Yoshikawa, H.; and Shino, K. (2009) Cell-based therapy in articular cartilage lesions of the knee. *Arthroscopy*, Vol25, No5, pp 531-52.
- Nöth U., Steinert A.F. and S.T. Rocky (2008). Technology Insight: Adult Mesenchymal Stem Cells for Osteoarthritis Therapy. *Nature Clinical Practice Rheumatology*, Vol4, No7, pp371-380.
- Noyes, F. R.; Bassett, R. W.; Grood, E. S.; and Butler, D. L. (1980) Arthroscopy in acute traumatic hemarthrosis of the knee. Incidence of anterior cruciate tears and other injuries. *J Bone Joint Surg Am*, Vol62, No5, pp687-95, 757.
- Ordemann R, Holig K, Wagner K, et al. (1998) Acceptance and feasibility of peripheral stem cell mobilisation compared to bone marrow collection from healthy unrelated donors. *Bone Marrow Transplant*, Vol 21, No Suppl 3, ppS25-8.
- Ossendorf, C.; Kaps, C.; Kreuz, P. C.; Burmester, G. R.; Sittinger, M.; and Erggelet, C. (2007) Treatment of posttraumatic and focal osteoarthritic cartilage defects of the knee with autologous polymer-based three-dimensional chondrocyte grafts: 2-year clinical results. *Arthritis Res Ther*, Vol9, No2, ppR41.
- Panagiota A.S., Sonia A. P., Maria S., Constantin N.B., Michael P. (2005). Characterization of the Optimal Culture Conditions for Clinical Scale Production of Human Mesenchymal Stem Cells. *Stem Cells Express* :DOI: 10.1634/stemcells.2004-0331

- Pacini S, Spinabella S, Trombi L, Fazzi R, Galimberti S, Dini F, Carlucci F, Petrini M. (2007) Suspension of bone marrow-derived undifferentiated mesenchymal stromal cells for repair of superficial digital flexor tendon in race horses. *Tissue Eng.* Vol13, No12, December 2007, pp2949-55.
- Peterson L, Minas T, Brittberg M, Nilsson A, Sjogren-Jansson E, Lindahl (2000). A. Two- to 9-year outcome after autologous chondrocyte transplantation of the knee. *Clinical Orthopaedics Related Research.* Vol 374, pp: 212-234.
- Pridie, K. H. (1959): A method of resurfacing osteoarthritic knee joints. *J Bone Joint Surg [Br]*, Vol41, pp 618-19.
- Sanchez, M.; Anitua, E.; Azofra, J.; Aguirre, J. J.; and Andia, I. (2008) Intra-articular injection of an autologous preparation rich in growth factors for the treatment of knee OA: a retrospective cohort study. *Clin Exp Rheumatol*, Vol26, No5, pp910-3, 2008.
- Saris DB, Vanlauwe J, Victor J, et al. (2009). Treatment of symptomatic cartilage defects of the knee: characterized chondrocyte implantation results in better clinical outcome at 36 months in a randomized trial compared to microfracture. *American Journal of Sports Medicine.* Vol 37, No Suppl 1, pp:10S-19S.
- Saw KY, Hussin P, Loke SC, Azam M, Chen HC, Tay YG, Low S, Wallin KL and Ragavanaidu K. (2009) Articular cartilage regeneration with autologous marrow aspirate and hyaluronic acid: an experimental study in a goat model. *Arthroscopy*, Vol25, No12, pp1391-1400.
- Saw KY, Anz A, Tay YG, Ragavanaidu K, Jee CSY and McGuire DA (2011) *Arthroscopy: The Journal of Arthroscopic and Related Surgery*, Vol 27, No 4, April 2011, pp 493-506
- Steadman JR, Rodkey WG, Briggs KK, Rodrigo JJ. (1999) The microfracture technique in the management of complete cartilage defects in the knee joint. *Orthopade* , Vol28, No1, pp26-32.
- Steadman, J. R.; Briggs, K. K.; Rodrigo, J. J.; Kocher, M. S.; Gill, T. J.; and Rodkey, W. G. (2003) Outcomes of microfracture for traumatic chondral defects of the knee: average 11-year follow-up. *Arthroscopy*, Vol19, No5, pp 477-84.
- Steinert, A. F.; Ghivizzani, S. C.; Rethwilm, A.; Tuan, R. S.; Evans, C. H.; and Noth, U. (2007) Major biological obstacles for persistent cell-based regeneration of articular cartilage. *Arthritis Res Ther*, Vol9, No3, pp213.
- Steinwachs, M. R.; Guggi, T.; and Kreuz, P. C. (2008) Marrow stimulation techniques. *Injury*, Vol39, No Suppl 1, pp S26-31.
- Strauss, E.; Schachter, A.; Frenkel, S.; and Rosen, J. (2009) The efficacy of intra-articular hyaluronan injection after the microfracture technique for the treatment of articular cartilage lesions. *Am J Sports Med*, Vol37, No4, pp720-6.
- Taylor SE, Smith RK, Clegg PD. (2007) Mesenchymal stem cell therapy in equine musculoskeletal disease: scientific fact or clinical fiction? *Equine Vet J.* Vol39, No2 March 2007, pp172-80
- Tuan, R. S. (2007) A second-generation autologous chondrocyte implantation approach to the treatment of focal articular cartilage defects. *Arthritis Res Ther*, Vol9, No5, pp109.
- Tytherleigh-Strong, G.; Hurtig, M.; and Miniaci, A. (2005) Intra-articular hyaluronan following autogenous osteochondral grafting of the knee. *Arthroscopy*, Vol21, No8, pp999-1005.

- Uccelli et al (2007). Mesenchymal Stem cells: a new strategy for immunosuppression. *Trends in Immunology*. Vol28, pp219-226.
- Violini S, Ramelli P, Pisani LF, Gorni C, Mariani P (2009) Horse bone marrow mesenchymal stem cells express embryo stem cell markers and show the ability for tenogenic differentiation by in vitro exposure to BMP-12. *BMC Cell Biol*. Vol22, April 2009, pp10:29.
- Wakitani S et al (2004). Autologous bone marrow stromal cell transplantation for repair of full thickness articular cartilage defects in human patellae: two case reports. *Cell transplantation*. Vol13,pp 595-600.
- Zeifang F, Oberle D, Nierhoff C, Richter W, Moradi B, Schmitt, H. (2010). Autologous Chondrocyte Implantation Using the Original Periosteum-Cover Technique Versus Matrix-Associated Autologous Chondrocyte Implantation: A Randomized Clinical Trial. *American Journal of Sports Medicine*. Vol 38, No 5, pp:924-933.

IntechOpen



## **Modern Arthroscopy**

Edited by Dr Jason L. Dragoo

ISBN 978-953-307-771-0

Hard cover, 302 pages

**Publisher** InTech

**Published online** 09, December, 2011

**Published in print edition** December, 2011

Modern Arthroscopy will assist practitioners to stay current in the rapidly changing field of arthroscopic surgery. The chapters in this book were written by a panel of international experts in the various disciplines of arthroscopy. The goals of this text are to present the classical techniques and teachings in the fields of Orthopaedics and Dentistry, but also to include new, cutting-edge applications of arthroscopy, such as temporomandibular arthroscopy and extra-articular arthroscopy of the knee, just to name a few. We hope Modern Arthroscopy becomes a core reference for your arthroscopic surgery practice.

### **How to reference**

In order to correctly reference this scholarly work, feel free to copy and paste the following:

Khay-Yong Saw, Adam Anz, Kathryne Stabile, Caroline SY Jee, Shahrin Merican, Yong-Guan Tay and Kunaseegaran Ragavanaidu (2011). Articular Cartilage Regeneration with Stem Cells, Modern Arthroscopy, Dr Jason L. Dragoo (Ed.), ISBN: 978-953-307-771-0, InTech, Available from:  
<http://www.intechopen.com/books/modern-arthroscopy/articular-cartilage-regeneration-with-stem-cells>

**INTech**  
open science | open minds

### **InTech Europe**

University Campus STeP Ri  
Slavka Krautzeka 83/A  
51000 Rijeka, Croatia  
Phone: +385 (51) 770 447  
Fax: +385 (51) 686 166  
[www.intechopen.com](http://www.intechopen.com)

### **InTech China**

Unit 405, Office Block, Hotel Equatorial Shanghai  
No.65, Yan An Road (West), Shanghai, 200040, China  
中国上海市延安西路65号上海国际贵都大饭店办公楼405单元  
Phone: +86-21-62489820  
Fax: +86-21-62489821



© 2011 The Author(s). Licensee IntechOpen. This is an open access article distributed under the terms of the [Creative Commons Attribution 3.0 License](https://creativecommons.org/licenses/by/3.0/), which permits unrestricted use, distribution, and reproduction in any medium, provided the original work is properly cited.

IntechOpen

IntechOpen